AD_____
(Leave blank)

Award Number: **W81XWH-10-1-0876**

TITLE: **Molecular Signatures and Diagnostic Biomarkers of Cumulative, Blast-Graded Mild TBI**

PRINCIPAL INVESTIGATOR: **Stanislav Svetlov, MD, PhD**

CONTRACTING ORGANIZATION:

Banyan Biomarkers, Inc.

Alachua, FL 32615
USA

REPORT DATE: October, **2012**

TYPE OF REPORT: **Annual**

PREPARED FOR: **U.S. Army Medical Research and Materiel Command**
Fort Detrick, Maryland 21702-5012

DISTRIBUTION STATEMENT:

X Approved for public release; distribution unlimited

☐ Distribution limited to U.S. Government agencies only; report contains proprietary information

The views, opinions and/or findings contained in this report are those of the author(s) and should not be construed as an official Department of the Army position, policy or decision unless so designated by other documentation.

REPORT DOCUMENTATION PAGE

Form Approved
OMB No. 0704-0188

1. REPORT DATE *(DD-MM-YYYY)*	2. REPORT TYPE	3. DATES COVERED *(From - To)*
19 October 2012	Annual	15 September 2011-14 September 2012

4. TITLE AND SUBTITLE

Molecular Signatures and Diagnostic Biomarkers of Cumulative, Blast-Graded Mild TBI

5a. CONTRACT NUMBER

5b. GRANT NUMBER
W81XWH-10-1-0876

5c. PROGRAM ELEMENT NUMBER

6. AUTHOR(S)
PI: Stanislav Svetlov, MD, PhD

5d. PROJECT NUMBER

5e. TASK NUMBER

5f. WORK UNIT NUMBER

7. PERFORMING ORGANIZATION NAME(S) AND ADDRESS(ES)

Banyan Biomarkers, Inc.

Alachua, FL 32615
USA

8. PERFORMING ORGANIZATION REPORT NUMBER

9. SPONSORING / MONITORING AGENCY NAME(S) AND ADDRESS(ES)
U.S. Army Medical Research and Materiel Command
Fort Detrick, Maryland 21702-5012

10. SPONSOR/MONITOR'S ACRONYM(S)

11. SPONSOR/MONITOR'S REPORT NUMBER(S)

12. DISTRIBUTION / AVAILABILITY STATEMENT

Approved for public release; distribution unlimited

13. SUPPLEMENTARY NOTES

14. ABSTRACT During 2-d year, we continued comparing blast load characteristics producing mild through severe TBI of 'composite' , accompanied with head acceleration with primary blast, in which peak overpressure 'flows the head through a rostral part of the brain w/o significant head acceleration' Also, we begun to fully characterize brain injury and biomarkers after repeated blast exposure by ELISA, antibody microarrays, and Western blot. Rats were subjected to a primary blast of 50-53 psi kPa overpressure and total duration of 75 μsec at the frontal part of the rat's skull. Portable cumulative blast sensors were placed on the head front and rat spine. Multiple blasts were performed as a series of 3 exposures, with a 45 min to 1 hr recovery between each blast. High speed imaging revealed a low degree of acceleration at rat position "off-axis" toward external shock tube. We measured blood accumulation of GFAP and CNPase, neuronal UCH-L1 and NSE, neuroendocrine peptide Orexin A, and Neuropilin-2 at 1 day and 7 days after a single and multiple blast exposures. Multiple blasts significantly augmented increased levels of GFAP, UCH-L1, NSE and NRP-2, but not Orexin A, vs. single 1 day post-blast, while at 7 days the cumulative effects of multiple blasts were much lower, if any. On the other hand, serum CNPase after multiple blasts was significantly augmented vs. single blast both at 1 day and 7 days post exposure. The improved prototype of cumulative blast sensor and signal conditioning circuit were tested at Banyan Biomarkers on 19 October 2012. Please see details and progress in the appendix.

15. SUBJECT TERMS
blast wave; brain injury; 'composite' blast; primary blast; Cumulative Blast and Impulse Exposure Sensing Package (CBI-ESP); GFAP; CNPase; NSE; L-selectin; Orexin A; NGF-beta; Neuropilin-2 (NRP-2)

16. SECURITY CLASSIFICATION OF:			17. LIMITATION OF ABSTRACT	18. NUMBER OF PAGES	19a. NAME OF RESPONSIBLE PERSON
					USAMRMC
a. REPORT	b. ABSTRACT	c. THIS PAGE	UU		19b. TELEPHONE NUMBER *(include area code)*
U	U	U			

Standard Form 298 (Rev. 8-98)
Prescribed by ANSI Std. Z39.18

Table of Contents

1. Frontiers in Neurol. 2012;3:15

2. Prima V , Scharf D, Gutierrez H, Kirk DR Svetlov A, Curley KC, Hayes RL, Svetlov SI MULTIPLE BLAST EXPOSURES ALTERS NEURO-GLIAL, NEUROENDOCRINE AND GROWTH FACTOR BIOMARKERS TO BLAST LOAD IN RATS
Poster presented at Advanced Technology Applications for Combat Casualty Care (ATACCC)/The Military Health System Research Symposium (MHSRS) August, 2012 Ft. Lauderdale

3. **Stanislav Svetlov**, Victor Prima, Daniel Kirk, Hector Gutierrez, Kenneth Curley, Ronald Hayes, Kevin Wang "Neuro-glial and systemic mechanisms of pathological responses to primary blast overpressure (OP) compared to 'composite' blast accompanied by head acceleration in rats" Paper published and presented at NATO Conference 'A Survey of Blast Injury across the Full Landscape of Military Science, October 2011, Halifax.
Proceeding of NATO conference HFN-207

4. Hector Gutierrez and Daniel Kirk for Banyan Biomarkers " Experimental Framework for Cumulative Blast Detection and Data Acquisition for Assessment of Blast-Related Injury in Animal Studies", **April 16, 2012 / October 21, 2012**

Introduction.

Objectives of the entire project are: (i) Develop an experimental framework for reproducing multiple blast wave exposures and recording multiple blasts in an animal model using a prototype sensor device, (ii) define cumulative blast load upon multiple blast exposures and distinguish pathophysiological mechanisms of mild through severe TBI to formulate blast load injury scale, (iii) identify and validate biochemical markers of cumulative blast exposures.

In year 1, we determined blast load characteristics producing mild through severe TBI and defined 'composite' and primary blast parameters. Schlieren optics technique was used to visualize blast wave interaction with experimental animal. The pathological effects of primary blast OP exposure of controlled duration, peak pressure and transmitted impulse were compared with brain injury by a severe blast load accompanied with strong head acceleration. We assessed and partially characterized brain injury signatures when primary blast wave hits frontal head with open or covered body vs. composite blast: neuro-glial injury evaluated by silver staining, and GFAP/CNPase and NSE. Biomarkers of neuro-glial injury GFAP, CNPase and NSE were accumulated in circulation in a particular time-dependent fashion. We developed a v1.1 of sensor package for detecting/recording a cumulative blast exposure, and begin to characterize mechanisms and biomarkers of brain injury in response to multiple mild/moderate blast exposures.

The objectives of **year 2** of the project has been (i) complete characterization severe/moderate TBI upon primary blast (peak overpressure) exposure compared to composite blast, (ii) continue developing a cumulative blast detecting/recording module, and (iii) characterizing biomarkers of TBI in response to multiple vs. single blast exposures. Multiple blasts significantly augmented increased levels of GFAP, UCH-L1, NSE and NRP-2, but not Orexin A, vs. single 1 day post-blast, while at 7 days the cumulative effects of multiple blasts were much lower, if any. On the other hand, serum CNPase after multiple blasts was significantly augmented vs. single blast both at 1 day and 7 days post exposure. The improved prototype of cumulative blast sensor and signal conditioning circuit were tested at Banyan Biomarkers on 19 October 2012.

BODY

In the body section, I present novel data and progress related to multiple blast biomarker responses. Recent issues pertinent to the development of cumulative blast sensor have been also briefly discussed. Detailed explanation and solutions of a sensor have been presented in FIT appendix. In addition, comparing biomarkers of moderate 'composite'blast TBI , accompanied with head acceleration with primary blast, in which peak overpressure 'flows the head through a rostral part of the brain w/o significant head acceleration', is presented in detail in published paper in Appendix.

SOW 2: Develop a cumulative blast detecting/recording module, and characterize pathophysiology of mTBI in response to multiple blast exposures. Define cumulative blast load upon multiple blast exposures and distinguish pathophysiological mechanisms of mild TBI to formulate blast load injury scale. (Months 2-24)

Task 3: Characterize and validate a portable cumulative blast detection device using novel MEMS chip technology (FIT). Assess detection of multiple blast exposures at different 3-D rat orientations to blast wave, and compare cumulative effects in rats using our existing modular system and portable device. (Months 2-18, in progress)

Diaphragm	External sensor R=2 in @ 43 deg from shock tube exit – (psi)
0.003 + 4 layer of tape	35 .12
0.004 + 4 layer of tape	43.53
0.005 + 4 layer of tape	54.74

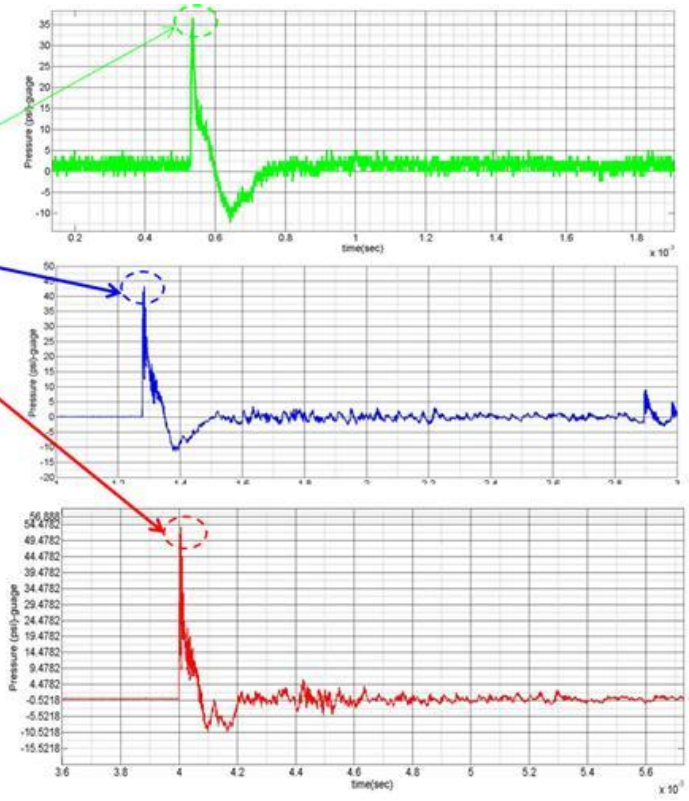

1. Maximum peak overpressure achieve with Banyan's current 1-inch shock tube.
Banyan's 1-inch shock tube can reach peak overpressure up to nearly 55 psi.
This has been consistently recorded and documented. We demonstrated that the use of successively thicker diaphragms, in combination with layers of tape used as sealant, provided increased peak overpressures as expected and shown in the table and plots above. Peak overpressure events last one to a few microseconds in near ideal blast waves (i.e., when the

effect of venting gas is almost completely eliminated). Advanced PXI-based data acquisition modules from FIT, at sample rates up to 50 Msamples/sec, were used to establish that to accurately capture peak overpressure events at sampling rate of at least 2.5 Msamples/second is needed.

The plots shown in previous page were sampled at 2.5 Msamples/sec (non-multiplexed) using a PXI-6132 14Bit, 2.5 MSample/sec/channel, simultaneous sampling multifunction data acquisition board. For the same reasons, it was also discovered during September session, that the currently existing data acquisition board on use at Banyan (DAQcard 6062E) sampling four multiplexed pressure sensors at 90 kSamples/sec, has a high chance of missing the peak overpressure event, and therefore fails recording the correct value of the peak overpressure.

1. Preliminary testing from blast events using the CBI-CSP (Cummulative blast injury sensing package) have been performed at Banyan using two sensors and one data capture board, as shown in the figures below:

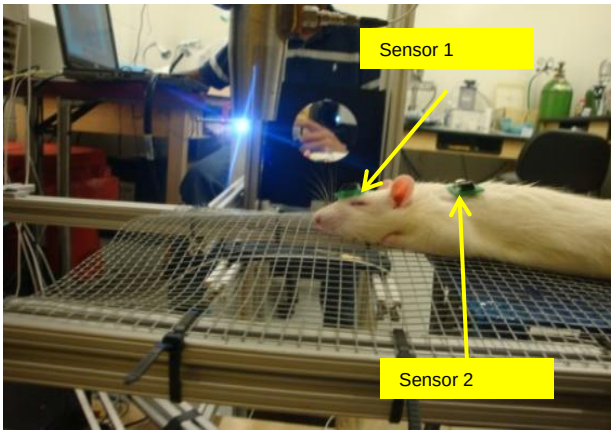

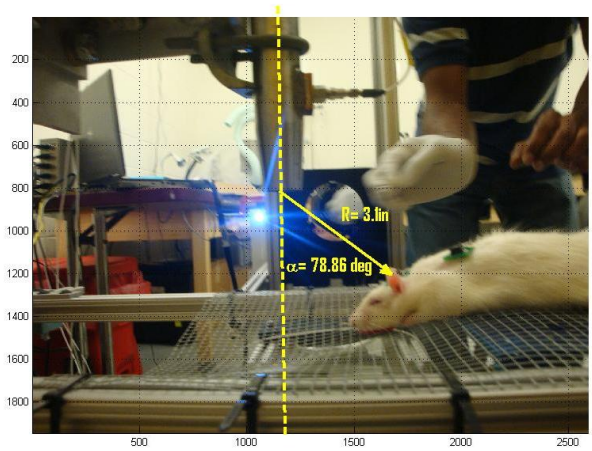

Test #	Sensor 1 (psi) peak Overpressure(psi)	Sensor 2 (psi) peak Overpressure(psi)	Location from exit of shock tube	Time
Test 1	19.15	17.15	R=3.13 in Angle =78.86 deg	
Test 2	18.24	16.25	R=3.19 in Angle=68.50deg	5 mins after Test 1
Test 3	20.28	16.19	R= 3.02 in A Angle=68.25 deg	20 mins after Test 2

Table 1 – Low pressure tests using CBI-CSP device. Diaphragm thickness = 0.003 inch, no tape.

The data in table 1 shows results recorded in the SD memory card attached to the CBI-CSP data capture board in three successive tests, for sensor locations 1 and 2, at “low pressure” (0.003 inch diaphragm with no sealant tape). More detailed results from all testing conducted that day at Banyan using the CBI-CSP device were included and discussed in the corresponding quarterly report (Table 2).

Specimen Number	Test Name	Mach number	Details	R	α	Sensor 1 (CSB-CSP)	Sensor 2 (CSB-CSP)
Specimen 1	rat1	2.12	SINGLE BLAST , HEAD EXPOSURE	2.01	46.33	NA	NA
Specimen 2	rat2	2.061	SINGLE BLAST , HEAD EXPOSURE	2.18	48.79	NA	NA
Specimen 3	rat3	2.03	SINGLE BLAST, FULL BODY EXPOSURE	2.20	55.19	NA	NA
Specimen 4	rat4	2.09	SINGLE BLAST, FULL BODY EXPOSURE	2.47	47.62	NA	NA
Specimen 5	rat5	2.16	SINGLE BLAST, FULL BODY EXPOSURE	2.08	49.44	NA	NA
Specimen 6	rat6	2.13	SINGLE BLAST, FULL BODY EXPOSURE	2.26	47.12	NA	NA
Specimen 7	rat7	2.17	1 BLAST EXPOSURE FULL BODY	2.11	46.15	NA	NA
	rat9	2.05	2nd BLAST EXPOSURE FULL BODY, 25 min from 1st blast	2.25	54.76	18.69	15.96
	rat11	2.09	3rd BLAST EXPOSURE FULL BODY, 28 min from 2nd blast	2.51	53.58	19.53	16.72
Specimen 8	rat8	2.16	1 BLASTEXPOSURE FULL BODY	2.22	59.91	18.66	16.46
	rat10	2.06	2nd BLAST EXPOSURE FULL BODY, 28 min from 1st blast	2.13	47.33	20.94	16.77
	rat12	2.13	3rd BLAST EXPOSURE FULL BODY, 24 min from 2nd blast	2.31	52.32	20.55	16.77
Specimen 9	rat13	2.17	1 BLAST EXPOSURE, FULL BODY	2.47	52.66	19.42	16.93
	rat15	2.04	2nd BLAST EXPOSURE FULL BODY, 15 min from 1st blast	2.01	58.43	18.16	15.96
	rat17	2.16	3rd BLAST EXPOSURE FULL BODY,18 min from 2nd blast	2.20	42.22	23.52	17.48
Specimen 10	rat14	2.14	1 BLAST EXPOSURE, FULL BODY	2.40	49.90	NA	NA
	rat16	2.24	2nd BLAST EXPOSURE FULL BODY, 20 min from 1st blast	2.20	46.22	22.99	17.19
	rat18	2.11	3rd BLAST EXPOSURE FULL BODY, 15 min from 2nd blast	2.10	43.18	22.75	17.24

Table 2. Summary table of high pressure testing using the CBI-CSP device on 01-July-11. Diaphragm thickness was 0.005 inch + 4 Layers of Tape

As shown in Page 1 of this document, a 0.003 inch diaphragm with no sealant tape should have produced an overpressure event with peak pressure near or above 30 psi at a location (R and α) as shown in Figures 1-2 in the previous page. Instead, the CBI-CSP consistently recorded peak pressures near 20 psi.

There are two possible reasons for that and solutions which are described in detail in FIT Appendices.

Briefly:

1. The maximum sampling rate of the analog to digital converter available on the CBI-CSP device at the time of these tests was 150 kSamples/sec/channel. While this is more than 50% better than the maximum sampling rate available on the DAQCard 6062E currently deployed at Banyan, it is still 17 times slower than the 2.5 Msamples/sec/channel that was later found adequate to accurately detect the peak overpressure values. Version 1 of the CBI-CSP device was designed before we had an accurate numerical and experimental assessment of the sampling rate required to accurately capture the peak overpressure event. Version 1 is the first version designed and released within our currently ongoing development contract, and as such it was deployed as a preliminary prototype for assessment and future improvement.

2. The type of pressure sensing device on board Version 1 of the CBI-CSP package is the calibrated MPXH6300A Integrated Silicon Pressure Sensor for absolute pressure, with on-chip signal conditioning and temperature compensation, from Freescale Corporation (http://www.freescale.com). The principle of operation of this sensor is shown below:

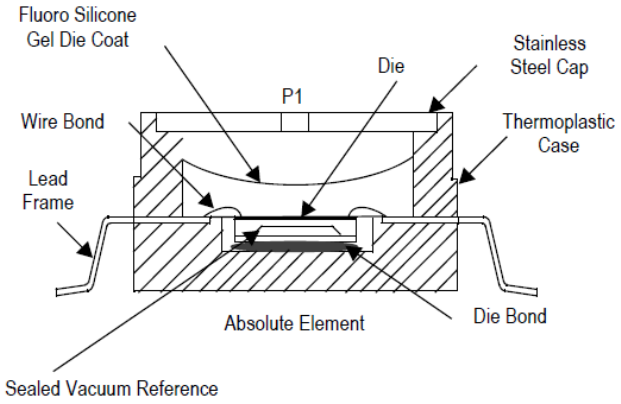

The type of sensing technology for pressure sensors to be used in the CBI-CSP device is highly limited due to size and weight restrictions of the application, in particular if the device must be small enough to be used in rodents. Under such restrictions, the use of piezoelectric pressure transducers is prohibitive in terms of weight and size due to their need of signal conditioning and the typical size and shape of piezoelectric piezo transducers.

Task 4: Assess brain injury characteristics upon exposure to repeated low level blast; determine cumulative blast load-injury correlations.

Next round of testing in rats was performed with the sensors calibrated using The test rig shown in Figure 7 below will be used during the next quaternary period to test the performance of both the proposed sensing elements and signal conditioner circuit with blast events created on the 1 inch shock tube at Florida Tech. The critical performance metric for both sensing elements and circuit prototype is the capacity to capture the correct peak overpressure value and time domain shape of the blast event, as compared to those measured using a laboratory-grade reference system.

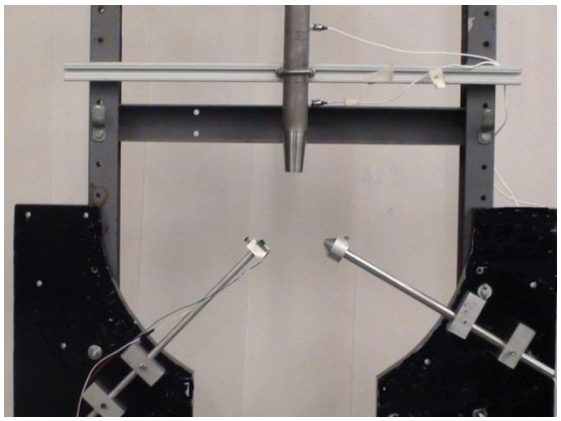

Figure 7. Experimental Test set up to compare pressure traces using the CBI-CSP pressure sensor and signal conditioner (left) versus a reference laboratory sensor (PCB pressure sensor Model Y102A) (right)

That provided the signal intensity and shape similar to the previous Banyan experimental series, resulting in effective Peak Overpressure 50-53 psi for 75 μsec.

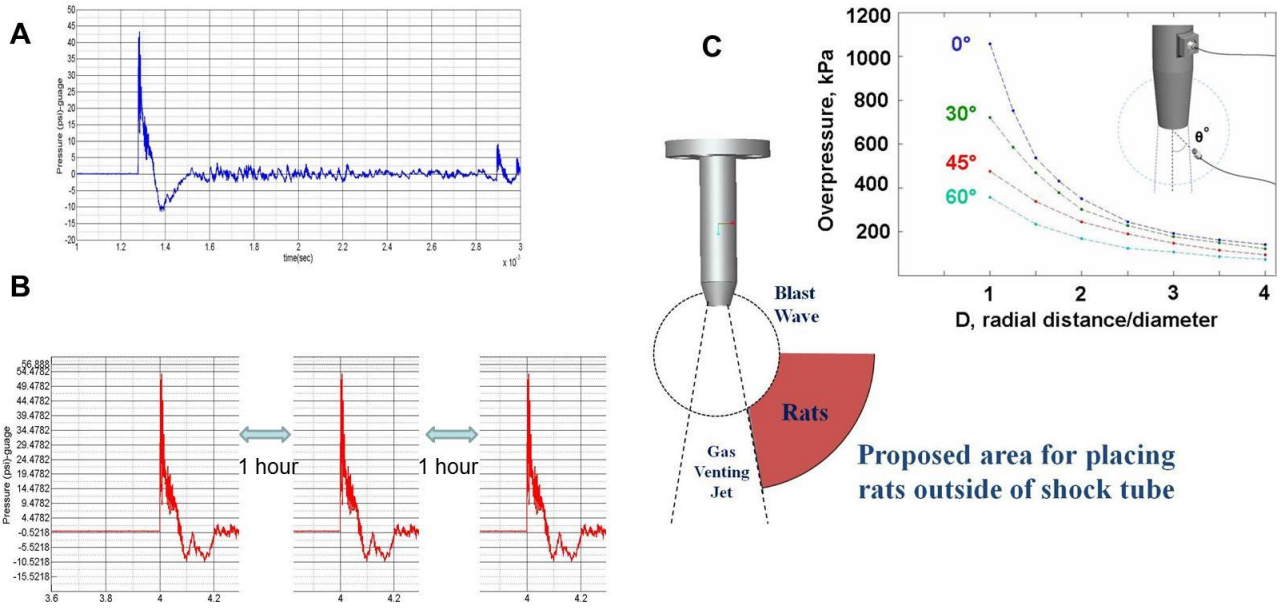

Representative overpressure traces during single (A) and multiple (B) blast exposures; (C) Blast wave overpressure as a function of radial distance and angle.

I. Neural-Glial TBI Markers released in Blood after Single/Multiple Blast:

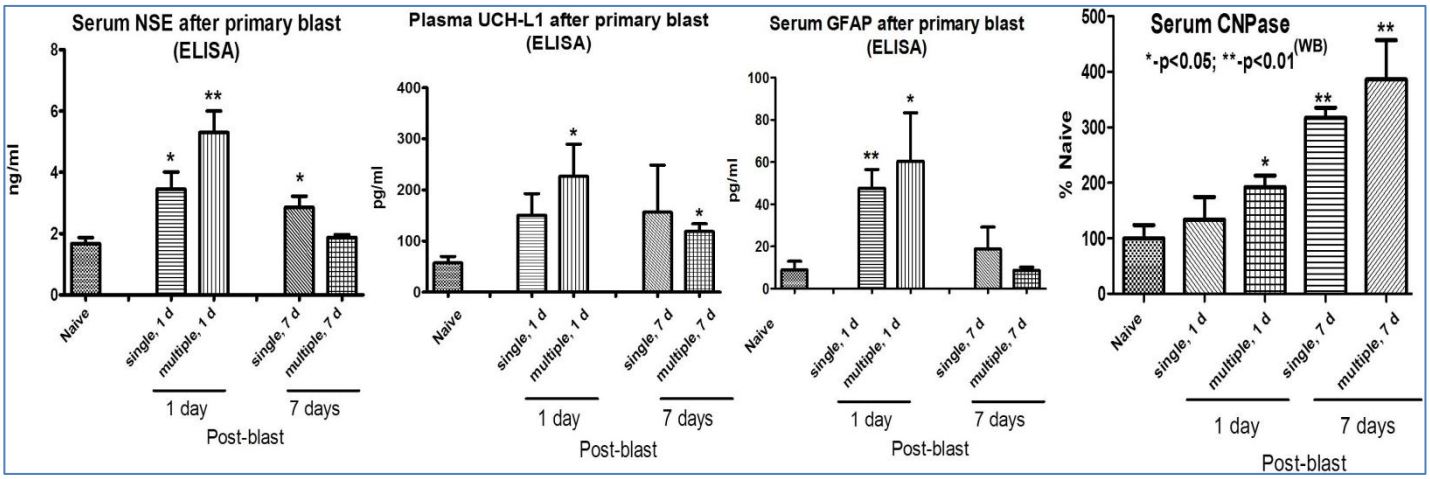

Rats were subjected to a primary blast of 50-53 psi kPa overpressure and total duration of 75 μsec at the frontal part of the rat's skull. Portable cumulative blast sensors were placed on the head front and rat spine. Multiple blasts were performed as a series of 3 exposures, with a 45 min to 1 hr recovery between each blast. High speed imaging revealed a low degree of acceleration at rat position "off-axis" toward external shock tube. Multiple blasts significantly augmented increased levels of GFAP, UCH-L1 and NSE vs single blast at 1 day post blast. No augmentation was found at 7 day post-blast. On the other hand, serum CNPase after multiple blasts was significantly augmented vs. single blast both at 1 day and 7 days post exposure. At least 4 rats were examined in each group. *-p<0.05; **-p<0.01

II. **Neuroendocrine, inflammatory and growth factor blast TBI Markers**

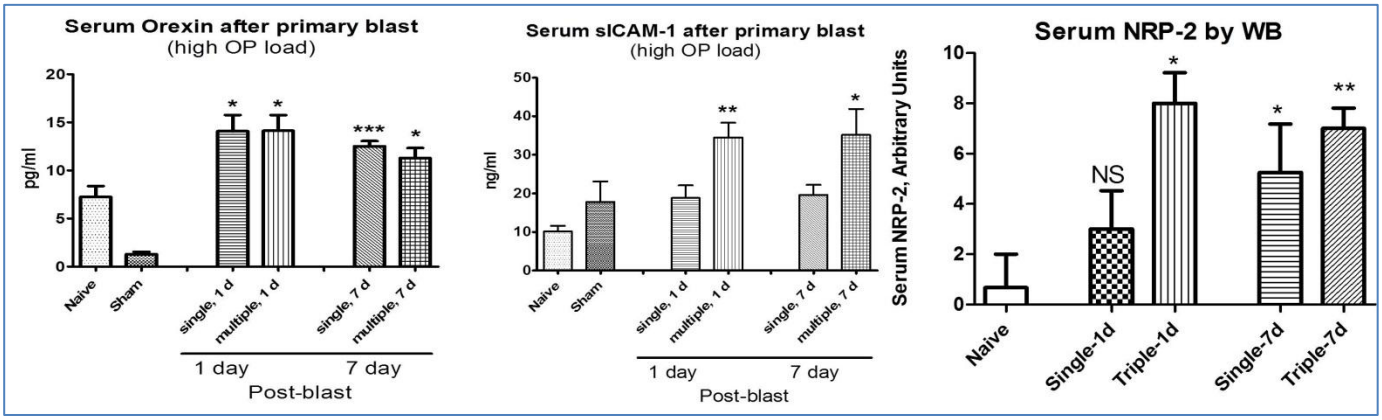

The conditions of rat exposures were as shown above for neuro-glial markers. Although Orexin A was dramatically elevated at day 1 and 7 post-blast, no differences in multiple blast responses vs. single were found. In contrast, both sICAM and NRP-2 serum levels after multiple blasts were higher than after single at day 1 and 7 post-blast. At least 4 rats were examined in each group. *-p<0.05; **-p<0.01

Finally, we compared Blood Brain Barrier (BBB) permeability following single and multiple blasts.

A 2% solution of Evans Blue Dye in PBS (4 mL/kg of body weight) was injected i.p. and the stain was allowed to circulate for 3 hours**.** At 4 hrs after first blast the anesthetized animals were intracardially perfused with PBS. Brain and liver samples were then isolated and weighed, homogenized in 2 ml 50% trichloroacetic acid per gram tissue and centrifuged. The absorbance of the extracted dye in supernatant at 620 nm was used to quantify the relative tissue content of EBD.

As can be seen, blast exposure induces Evans Blue Dye accumulation in brain but not in the liver. Moreover, multiple blast further augmented the Dye accumulation suggesting that BBB has a tendency and ability to reopen after repeated blast exposures.

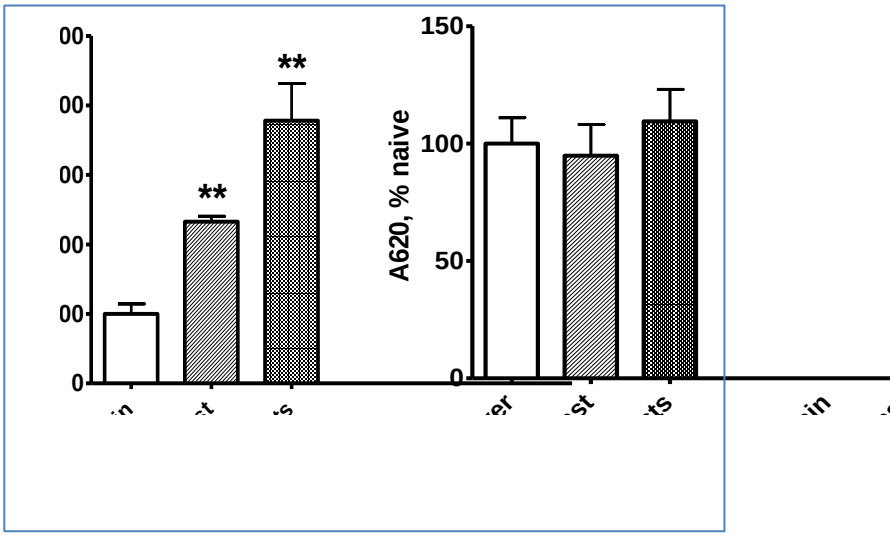

BBB Permeability after Blast

Key Research Accomplishments:

- Further detailed comparison of moderate 'Primary' and 'Composite' blast responses revealed the differences in pathogenic pathways and biomarker patterns. While both type of exposures were characterized by strong gliosis, 'composite' blast on the head (accompanied by head acceleration) produces significantly higher neuronal injury.

- Systemic, vascular, neuroinflammatory and neuroendocrine responses are essential components in responses to blast:

    - Orexin A, sICAM and Neuropilin-2 (NRP-2) appear to be the most prominent biomarkers

- The FIT prototype sensor and signal conditioning circuit have been designed, built and successfully tested. The proposed prototype has demonstrated enough response speed to accurately record the peak overpressure of the blast event as compared to the benchmark PCB sensor.

- Different biomarkers exhibited significantly different response to a single vs. multiple blast:

    - Although Orexin A was dramatically elevated at day 1 and 7 post-blast, no differences in multiple blast responses vs. single were found. In contrast, both sICAM and NRP-2 serum levels after multiple blasts were higher than after single at day 1 and 7 post-blast.

    - Multiple blasts significantly augmented increased levels of GFAP, UCH-L1 and NSE vs single blast at 1 day post blast. No augmentation was found at 7 day post-blast. On the other hand, serum CNPase after multiple blasts was significantly augmented vs. single blast both at 1 day and 7 days post exposure.

    - Multiple blast further augmented the Dye accumulation suggesting that BBB has a tendency and ability to reopen after repeated blast exposures.

Reportable Outcomes for the project period September 16, 2011-September 15, 2012

1. The paper invited for special topic Blast-induced Neurotrauma and entitled "**Neuro-glial and systemic mechanisms of pathological responses in rat models of primary blast overpressure compared to "composite" blast.**" by Svetlov SI, Prima V, Glushakova O, Svetlov A, Kirk DR, Gutierrez H, Serebruany VL, Curley KC, Wang KK, Hayes RL. has been published in Frontiers in Neurol. 2012;3:15. Epub 2012 Feb 9**,see Appendices**

2. Abstract and poster entitled 'MULTIPLE BLAST EXPOSURES ALTERS NEURO-GLIAL, NEUROENDOCRINE AND GROWTH FACTOR BIOMARKERS TO BLAST LOAD IN RATS" by Prima V1 , Scharf D1, Gutierrez H2, Kirk DR2 Svetlov A1, Curley KC3, Hayes RL1, Svetlov SI was presented at Advanced Technology Applications for Combat Casualty Care (ATACCC)/ The Military Health System Research Symposium (MHSRS) August, 2012 Ft. Lauderdale, **see Appendices**

3. Presentation and published paper entitled "**Neuro-glial and systemic mechanisms of pathological responses to primary blast overpressure (OP) compared to 'composite' blast accompanied by head acceleration in rats" by Stanislav Svetlov**, Victor Prima, Daniel Kirk, Hector Gutierrez, Kenneth Curley, Ronald Hayes, Kevin Wang was presented at NATO Conference 'A Survey of Blast Injury across the Full Landscape of Military Science, October 2011, Halifax. Proceeding of NATO conference HFN-207 **see Appendices**

Conclusion

In the first year of the project, we generally validated the models of primary blast load vs. 'composite' blast exposure accompanied by head acceleration. Schlieren optics technique was used to visualize blast wave interaction with experimental animal. Blast parameters (peak overpressure, duration, and impulse power) on the surface of rats at various orientations to the blast wave were determined and standardized.

During second year, we continued comparing blast load characteristics producing mild through severe TBI of 'composite' , accompanied with head acceleration with primary blast, in which peak overpressure 'flows the head through a rostral part of the brain w/o significant head acceleration' Also, we begun to fully characterize brain injury and biomarkers after repeated blast exposure by ELISA, antibody microarrays, and Western blot.
Rats were subjected to a primary blast of 50-53 psi kPa overpressure and total duration of 75 μsec at the frontal part of the rat's skull. Multiple blasts were performed as a series of 3 exposures, with a 45 min to 1 hr recovery between each blast.

We measured blood accumulation of GFAP and CNPase, neuronal UCH-L1 and NSE, neuroendocrine peptide Orexin A, and Neuropilin-2 at 1 day and 7 days after a single and multiple blast exposures. Multiple blasts significantly augmented increased levels of GFAP, UCH-L1, NSE and NRP-2, but not Orexin A, vs. single 1 day post-blast, while at 7 days the cumulative effects of multiple blasts were much lower, if any. On the other hand, serum CNPase after multiple blasts was significantly augmented vs. single blast both at 1 day and 7 days post exposure. In addition, multiple blasts increased BBB opening as compared to a single blast exposures, suggesting that BBB has a tendency and ability to reopen after repeated blast exposures.

The FIT prototype sensor and signal conditioning circuit have been designed, built and successfully tested. The proposed prototype has demonstrated enough response speed to accurately record the peak overpressure of the blast event as compared to the benchmark PCB sensor. Further tests on an improved test rig will help to further demonstrate the performance of the FIT sensor using a better method to accurately place both sensors in the field of the blast relative to each other and to the blast axis.

The last component missing in the proposed CBI-ESP device (cumulative blast and impulse electronic sensing package) is a new data logger capable to provide sampling rate up to 1 MHz in a package no larger than 1 inch square. This is the focus of the next performance period of this subcontract.

References:

1. **Svetlov SI,** Larner SF, Kirk DR, Atkinson J, Hayes RL, Wang KK. has been published *J Neurotrauma* 2009 Jun, 26:1-9

2. **Svetlov SI,** Prima V, Kirk DR, Gutierrez H, Curley KC, Hayes RL, Wang KK. Morphologic and Biochemical Characterization of Brain Injury in a Model of Controlled Blast Overpressure Exposure. J Trauma. 2010 Oct;69(4):795-804

2a. **Svetlov SI,** Prima V, Kirk DR, Gutierrez H, Curley KC, Hayes RL, Wang KKW. Neuro-glial and systemic mechanisms of pathological responses to primary blast overpressure (OP) compared to 'composite' blast accompanied by head acceleration in rats. In: Proceeding of NATO conference 'A Survey of Blast Injury across the Full Landscape of Military Science, 2011.

3. Stuhmiller JH, Ho KH, Vander Vorst MJ, et al. A model of blast overpressure injury to the lung. *J Biomech* 1996;29:227-234.

4. Jaffin JH, McKinney L, Kinney RC, et al. A laboratory model for studying blast overpressure injury. *J Trauma* 1987;27:349-356.

5. Atkinson JP, Faure JM, Kirk DR, et al. Generation and Analysis of Blast Waves from a Compressed Air-Driven Shock Tube. The American Institute of Aeronautics and Astronautics (AIAA) Journal 2010;In press.

6. Guy RJ, Kirkman E, Watkins PE, et al. Physiologic responses to primary blast. *J Trauma* 1998;45:983-987.

7. Cooper PW. Explosives Engineering. Wiley-VCH; 1996.

8. Saljo A, Bao F, Haglid KG, et al. Blast exposure causes redistribution of phosphorylated neurofilament subunits in neurons of the adult rat brain. J Neurotrauma 2000;17:719-726.

9. Elsayed NM. Toxicology of blast overpressure. Toxicology 1997;121:1-15.

10. Stuhmiller JH. Biological response to blast overpressure: a summary of modeling. Toxicology 1997;121:91-103.

11. Svetlov SI, Larner SF, Kirk DR, et al. Biomarkers of Blast-Induced Neurotrauma: Profiling Molecular and Cellular Mechanisms of Blast Brain Injury. *J Neurotrauma* 2009, 26:1-9

12. de Olmos JS, Beltramino CA, de Olmos de Lorenzo S. Use of an amino-cupric-silver technique for the detection of early and semiacute neuronal degeneration caused by neurotoxicants, hypoxia, and physical trauma. *Neurotoxicol Teratol* 1994;16:545-561.

13. Switzer RC, 3rd. Application of silver degeneration stains for neurotoxicity testing. *Toxicol Pathol* 2000;28:70-83.

14. Kupina, N.C., Nath, R., Bernath, E.E., Inoue, J., Mitsuyoshi, A., Yuen, P.W., Wang, K.K., and Hall, E.D. (2001). The novel calpain inhibitor SJA6017 improves functional outcome after delayed administration in a mouse model of diffuse brain injury. J Neurotrauma *18*, 1229-1240.

13. Galea, E., P. Dupouey and D. L. Feinstein (1995). "Glial fibrillary acidic protein mRNA isotypes: expression in vitro and in vivo." J Neurosci Res **41**(4): 452-461.

14. Urrea C, Castellanos DA, Sagen J, et al. Widespread cellular proliferation and focal neurogenesis after traumatic brain injury in the rat. *Restor Neurol Neurosci* 2007;25:65-76.

15 Nylen K, Ost M, Csajbok LZ, et al. Increased serum-GFAP in patients with severe traumatic brain injury is related to outcome. *J Neurol Sci* 2006;240:85-91.

16. Kaur, C., J. Singh, M. K. Lim, B. L. Ng and E. A. Ling (1997a). "Macrophages/microglia as 'sensors' of injury in the pineal gland of rats following a non-penetrative blast." Neurosci Res **27**(4): 317-322.

frontiers in
NEUROLOGY

ORIGINAL RESEARCH ARTICLE
published: 09 February 2012
doi: 10.3389/fneur.2012.00015

Neuro-glial and systemic mechanisms of pathological responses in rat models of primary blast overpressure compared to "composite" blast

Stanislav I. Svetlov[1,2]*, Victor Prima[1]*, Olena Glushakova[1], Artem Svetlov[1], Daniel R. Kirk[3], Hector Gutierrez[3], Victor L. Serebruany[4], Kenneth C. Curley[5], Kevin K. W. Wang[6] and Ronald L. Hayes[1]

[1] *Banyan Laboratories, Inc, Alachua, FL, USA*
[2] *Department of Medicine, University of Florida, Gainesville, FL, USA*
[3] *Department of Mechanical and Aerospace Engineering, Florida Institute of Technology, Melbourne, FL, USA*
[4] *Heart Drug Research LLC, Towson, MD, USA*
[5] *United States Army Medical Research and Materiel Command, Fort Detrick, MD, USA*
[6] *Department of Psychiatry, University of Florida, Gainesville, FL, USA*

Edited by:
Ibolja Cernak, Johns Hopkins University, USA

Reviewed by:
Jeffrey J. Bazarian, University of Rochester, USA
Eng Lo, Harvard University, USA

****Correspondence:***
Stanislav I. Svetlov and Victor Prima, Banyan Laboratories, Inc., 12085 Research Drive, Alachua, FL 32615, USA.
e-mail: ssvetlov@banyanbio.com; vprima@banyanbio.com

A number of experimental models of blast brain injury have been implemented in rodents and larger animals. However, the variety of blast sources and the complexity of blast wave biophysics have made data on injury mechanisms and biomarkers difficult to analyze and compare. Recently, we showed the importance of rat position toward blast generated by an external shock tube. In this study, we further characterized blast producing moderate traumatic brain injury and defined "composite" blast and primary blast exposure set-ups. Schlieren optics visualized interaction between the head and a shock wave generated by external shock tube, revealing strong head acceleration upon positioning the rat on-axis with the shock tube (composite blast), but negligible skull movement upon peak overpressure exposure off-axis (primary blast). Brain injury signatures of a primary blast hitting the frontal head were assessed and compared to damage produced by composite blast. Low to negligible levels of neurodegeneration were found following primary blast compared to composite blast by silver staining. However, persistent gliosis in hippocampus and accumulation of GFAP/CNPase in circulation was detected after both primary and composite blast. Also, markers of vascular/endothelial inflammation integrin alpha/beta, soluble intercellular adhesion molecule-1, and L-selectin along with neurotrophic factor nerve growth factor-beta were increased in serum within 6 h post-blasts and persisted for 7 days thereafter. In contrast, systemic IL-1, IL-10, fractalkine, neuroendocrine peptide Orexin A, and VEGF receptor Neuropilin-2 (NRP-2) were raised predominantly after primary blast exposure. In conclusion, biomarkers of major pathological pathways were elevated at all blast set-ups. The most significant and persistent changes in neuro-glial markers were found after composite blast, while primary blast instigated prominent systemic cytokine/chemokine, Orexin A, and Neuropilin-2 release, particularly when primary blast impacted rats with unprotected body.

Keywords: blast, brain injury, biomarkers, rat models, neuro-glia damage, systemic responses

INTRODUCTION

The nature of twenty-first century warfare has led to a significant increase in human exposure to blast overpressure (OP) impulses, which result in a complex of neuro-somatic disorders, including traumatic brain injury (TBI). Blast-related casualties outnumber conventional injuries during the last several years in Iraq and Afghanistan, while blast itself is being termed "the fourth weapon of mass destruction" (Born, 2005). Moreover, for every blast-related fatality, many more soldiers suffer multiple, low level non-lethal blast exposures. This often leads to mild traumatic brain injury (mTBI), which is rarely recognized in a timely manner and has become a signature injury of the Iraq and Afghanistan conflicts (Warden, 2006; Jones et al., 2007; Terrio et al., 2009). Symptoms of mild or moderate blast brain injury often do not manifest themselves until sometime after the injury has occurred (Cernak et al., 1999, 2011; Yilmaz and Pekdemir, 2007; Cernak and Noble-Haeusslein, 2010) and go undiagnosed and untreated because emergency medical attention is directed toward more visible injuries, such as penetrating flesh wounds (Belanger et al., 2005; Nelson et al., 2006; Wolf et al., 2009). However, even mild and moderate brain injuries can produce significant deficits and, particularly when repeated, can lead to sustained neuro-somatic damage and neurodegeneration (Cernak and Noble-Haeusslein, 2010). Thus, identifying pathogenic mechanisms and biochemical markers of blast brain injury in relevant experimental models is vital to the development of diagnostics for mTBI through severe TBI.

However, because of the design inconsistency of blast/shock generators used in the different studies, incomplete understanding of blast wave biophysics associated with real explosives vs. those produced by air or gas-driven shock tubes, and the details of wave interaction with model animals, disparities between laboratory models and data on brain injury mechanisms and putative biomarkers have been difficult to analyze and compare (Jaffin et al., 1987; Elsayed, 1997; Guy et al., 1998b; Chavko et al., 2009; Gyorgy et al., 2011, see Bass et al., 2012 for review). Moreover, pathogenic pathways and molecular signatures of neural responses and injurious effects of blast exposures remain elusive. Recently, we developed and employed a model of "composite" blast exposure with controlled parameters of blast wave impact and brain injury in rats (Svetlov et al., 2010). Our studies demonstrated the importance of positional orientation of the head and whole body of rats toward a blast wave generated from an external shock tube (Svetlov et al., 2011). Data from several laboratories including our studies (Svetlov et al., 2010, 2011) suggest that the mechanisms underlying blast-induced injuries, particularly mild/moderate, appear to be distinct from those imposed by mechanical impact or acceleration, and may involve the prominent systemic response (please see Cernak, 2010 for review).

The main objective of this study was to compare the effects of moderate peak overpressure exposure (primary blast) with brain injury produced by a severe/moderate blast accompanied by strong head acceleration (composite blast). The high speed imaging using Schlieren optic demonstrated blast wave interaction with the animal's head/body and revealed a negligible degree of acceleration at a position "off-axis" with the shock tube (primary blast wave exposure) compared to the "on-axis" experimental setup, which was accompanied by strong head/cervical acceleration generated by peak OP + venting gas (composite blast, or primary blast wave plus gas jetting phenomena). The specific dynamics of systemic, vascular inflammatory, and neuro-glial injury signatures, including neuron-specific enolase (NSE)/ubiquitin C-terminal hydrolase L1 (UCH-L1), GFAP, and CNPase biomarkers in serum, were established and characterized. For major pathway signatures and biomarkers, the detected levels raised at all the set-ups studied. However, the most significant and persistent changes in neuro-glial markers were found after composite blast, while primary blast instigated prominent systemic/vascular reactions, particularly when the whole animal body was subjected to blast wave.

MATERIALS AND METHODS

HARDWARE DESIGN AND SETUP

The compressed air-driven shock tube capable of generating a wide range of controlled blast waves was described in details previously (Svetlov et al., 2010). The tube consists of two sections: high pressure (driver) and low-pressure (driven) separated by a diaphragm. Peak overpressure, composition, and duration of the generated high pressure shockwaves are determined by the shock tube configuration including thickness, type of diaphragm material, driver/driven ratio, and the initial driver pressure at the moment of diaphragm rupture. In the presented series of experiments to explore the effects of different components of the blast/shock waves on the targeted animal brain we employed different spatial set-ups as described below. The blast pressure data was acquired using PCB piezoelectric blast pressure transducers and LabView 8.2 software. A National Instruments 1.25 M samples/s data acquisition card was used to acquire data from multiple channels. The rat head images during the blast event were captured at 40,000 frames/s using a high speed video camera (Phantom V310, Vision Research, Wayne, NJ, USA) and mirror-based Schlieren optics.

ANIMAL EXPOSURE TO A CONTROLLED BLAST WAVE

All experimental procedures in rats, including post-blast euthanasia, tissue, and blood collection were performed under guidelines and upon approval by the IACUC of the University of Florida and the ACURO office of the Department of Defense. Modeling of the primary blast and the "composite" overpressure load was achieved by variable positioning of the target vs. blast generator. All rats were anesthetized with isoflurane inhalations described previously in detail. After reaching a deep plane of anesthesia, they were placed into a holder exposing either only their head (body-armored setup) or whole body at the distance 5 cm below the exit nozzle of the shock tube. Rats were positioned either directly on the shock tube axis or at the 45° angle to it to expose them correspondingly to the "composite" blast including the compressed air jet or only to the primary blast wave (**Figure 1D**). Animals were then subjected to a single blast with a mean peak overpressure at the target of 230–380 kPa (**Figures 1A,B**). The exact static and dynamic overpressure values depending on the angle and distance of rat head from the nozzle of shock tube were established during the prior calibration tests (**Figure 1C**). The control group of animals underwent the same treatment (anesthesia, handling, recovery) except they were not exposed to blast.

BLOOD AND TISSUES COLLECTION

At the required time points following blast exposure, animals were euthanized, blood was withdrawn directly from the heart under isoflurane anesthesia and brain tissue samples were collected, snap-frozen in liquid nitrogen and stored at −70°C until further analysis. Immunohistochemical analysis. At 1 and 7 days after TBI (primary, head-only blast) animals were euthanized with lethal dose of pentobarbital, transcardially perfused with 4% paraformaldehyde and whole brains were removed, processed, and embedded in paraffin. Immunohistochemistry analysis was performed on paraffin-embedded 6 μm brain sections. Slides were de-paraffinized, incubated for 10 min at 95°C in Trilogy solution (Cell Marque, Rocklin, CA, USA) for antigen retrieval, blocked for endogenous peroxides, and incubated with primary antibodies for GFAP (Cell Signaling Technology, Danvers, MA, USA) or CNPase (Abcam, Cambridge, MA, USA) overnight at 4°C followed by treatments with secondary antibodies. The staining was visualized with 3,3′-diaminobenzidine (DAB; Dako, Carpinteria, CA, USA) for brown color development. Sections were counterstained with Hematoxylin (Dako). Negative controls were performed by treatment with species-matched secondary antibodies only (not shown). The slides were scanned and examined using Aperio ScanScope GL system with either 5× or 20× objective and ScanScope software.

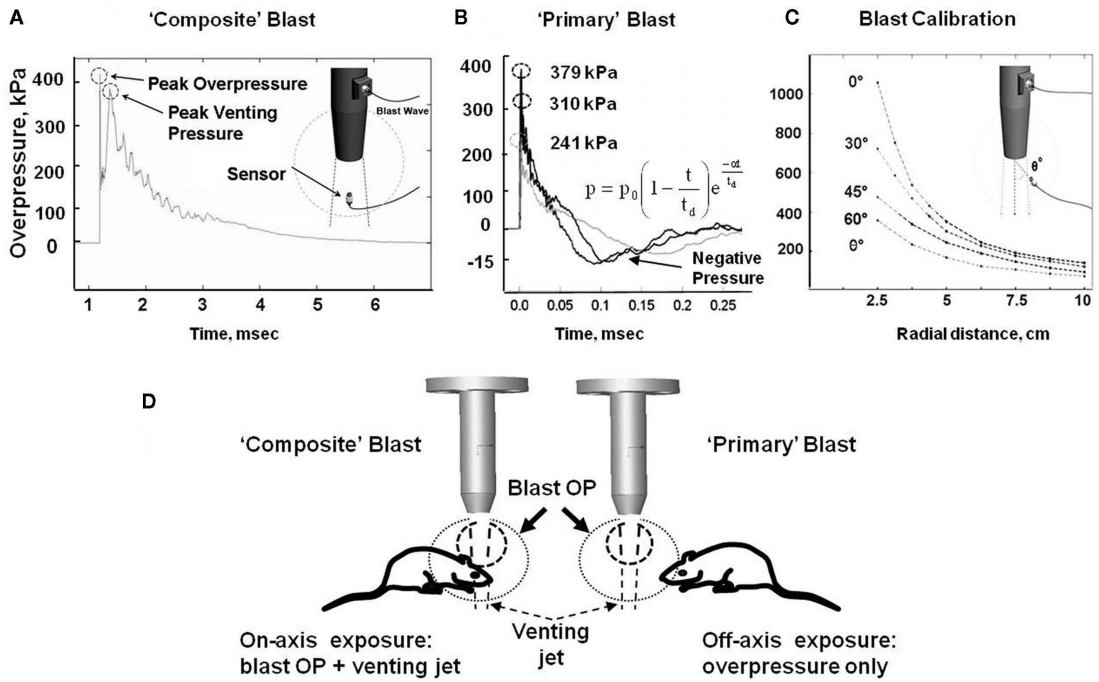

FIGURE 1 | Schematic presentation of blast exposure modeling in rats. (A) Overpressure recording on shock tube axis at 5 cm from the nozzle. **(B)** Overpressure recording with external "pencil" PCB at 5 cm and 45° from shock tube nozzle at three different diaphragm configurations. **(C)** Calibration of pressure on rat head depending on the angle and distance from the nozzle of shock tube. **(D)** Different shock tube set-ups to model "primary" and "composite" blast. Inset formula in **(B)** an empirical expression for the pressure decay with time at a fixed distance is characterized by a decay parameter α Kinney (1985).

SILVER STAINING ASSESSMENT OF NEURODEGENERATION IN RAT BRAIN

Neuroinjury and neurodegeneration was examined in the perfused and fixed brains using silver staining histochemical procedures according to Neuroscience Associates (Knoxville, TN, USA) utilizing the de Olmos Amino Cupric Silver Stain as previously described in detail (Svetlov et al., 2010). In addition, silver staining Kit from FD NeuroTechnologies (Ellicott City, MD, USA) was used where indicated. Rats were subjected to (i) "composite" head-directed severe blast exposure (358 kPa/10 ms total) on-axis (body protected); (ii) primary blast-off-axis exposure to peak overpressure only (233 kPa/113 μs total); and (iii) controlled cortical impact (CCI) of 2.0 mm depth performed as described previously (Liu et al., 2010).

WESTERN BLOT ANALYSIS OF BRAIN TISSUES

For Western blot analyses tissue samples were prepared, separated by SDS-polyacrylamide gel electrophoresis and electro-blotted onto polyvinylidene difluoride membranes as described previously in detail (Svetlov et al., 2010). After overnight incubation with primary antibodies for CNPase or Neuropilin-2 (Cell Signaling Technology, Danvers, MA, USA) proteins were incubated with conjugated secondary antibodies and detected by either colorimetric or chemiluminescent (ECL) detection system. Actin was used as a loading control and bands of interest were normalized for actin expression. Semi-quantitative assessment of protein levels by western blot densitometry was conducted using NIH ImageJ image processing program.

Protein ELISA assays. Commercially available Sandwich ELISA (SW ELISA) kits for GFAP (BioVendor, Candler, NC, USA), NSE (Life Sci. Advanced Tech., St. Petersburg, FL, USA), β-NGF; Abnova, Walnut, CA, USA), Orexin A (Uscn Life Sci., Wuhan, P. R. China), L-selectin (CUSABIO Biotech, Wuhan, P. R. China) and soluble intercellular adhesion molecule-1 (sICAM-1; CUSABIO Biotech) were used according to the manufacturer's instructions. UCH-L1 in CSF and plasma was quantitatively detected using proprietary SW ELISA (Banyan Biomarkers, Inc.) and recombinant UCH-L1 as standard.

ANTIBODY ARRAY ASSAYS

Custom Biotin Label-based (L-series) Rat Antibody array (RayBiotech, Norcross, GA, USA) was used to assess relative levels of Interleukin-1, Interleukin-10, Neuropilin-2, Fractalkine, and Integrin α/β in rat serum following blast exposure.

STATISTICS

Statistical analyses were performed using GraphPad Prism 5 software. Values are means ± SEM. Data were evaluated by two-tailed unpaired *t*-test with or without Welch corrections where indicated.

RESULTS

RAT MODELS OF BLAST EXPOSURE USING EXTERNAL SHOCK TUBE: PRIMARY BLAST LOAD VS. "COMPOSITE" BLAST EXPOSURE

Our shock tube was designed and built to model a freely expanding blast wave as generated by a typical explosion. Both static and

dynamic (total) pressures were measured as functions of angle and radial distance from shock tube exit using piezoelectric blast pressure transducers positioned at the target (**Figure 1C**). The pressure transducers registered three distinct events: (i) peak OP, (ii) gas venting jet-on-axis only, and (iii) negative pressure phase-off-axis only (**Figures 1A,B**). The exhaust of venting gas apparently distorted propagation of the blast wave and no negative phase was registered when dynamic pressure was measured on-axis of shock tube (**Figure 1A**), while a distinct and substantial negative phase (15–20 kPa) was detected off-axis (**Figure 1B**). Peak OP, positive phase duration, and impulse appear to be the key parameters that correlate to injury and likelihood of fatality in animals and humans, for various orientations of the specimen relative to the blast wave. A schematic of a shock tube nozzle and the alternative rat locations relative to the shock tube axis, blast OP wave, and gas venting cone is shown in **Figure 1D**. Shock tubes produce a "venting gas jet" immediately after the blast wave forms, substantially contaminating the blast wave in the direction of the shock tube axis (**Figure 1D**). In a composite blast setup, venting gas jet lasts the longest (up to ∼3–5 ms), albeit lower in magnitude than peak overpressure, represents the bulk of blast impulse, and possibly produces the most devastating impact. Schlieren optics (**Figure 2A**) demonstrated a strong downward head acceleration following the passage of peak overpressure which lasts 50–100 μs. However, cranial deformation was more severe during the gas venting phase, lasting up to 5 ms. This effect was eliminated by placing rats off-axis from the venting jet in a way that the main effect acting on the specimen is the peak overpressure event. The high speed recording coupled with Schlieren optical system visualized interaction of the blast wave with the animal head/body and revealed a negligible degree of acceleration at rat positioning "off-axis" toward shock tube (primary blast; **Figure 2B**). The pressure on the surface of rats was calibrated depending on the distance and angle from the nozzle of shock tube (**Figure 1C**).

NEURAL INJURY AND GLIOSIS IN RAT BRAIN AFTER DIFFERENT BLAST EXPOSURES ASSESSED BY SILVER STAINING AND IMMUNOHISTOCHEMISTRY

As can be seen in **Figure 3**, composite blast (on-axis) produces silver accumulation at the seventh day post-blast (**Figures 3A,D**), particularly in the hippocampus (indicated by arrows). CCI also results in positive staining in ipsilateral cortex and hippocampus (**Figures 3C,F**). In contrast, there was a rare occurrence of silver accumulation observed in the cortex or hippocampus after exposure to primary blast (**Figures 3B,E**; indicated by arrowheads).

Time-dependent expression of GFAP and CNPase characteristic for astrocytes and oligodendrocytes, respectively was studied by IHC after moderate composite on-axis blast (358 kPa/∼10 ms) with strong head acceleration or moderate primary off-axis blast (234 kPa/113.8 μs positive phase) with minor head acceleration (**Figure 4**). These data suggest that both primary and "composite" blasts strongly induce astrogliosis (GFAP, **Figure 4**: upper panel) and oligodendrocytosis (CNPase, **Figure 4**: lower panel) in rat hippocampus evident as early as 1 day and lasting up to 7 days post-blast.

SERUM LEVELS OF BIOMARKERS OF NEURO-GIAL INJURY FOLLOWING BLAST EXPOSURE

To asses if markers of neuronal injury are released into circulation, we assayed serum levels of NSE and UCH-L1 after different blast exposures (**Figure 5**). As shown in **Figure 5A**, remarkable accumulation of NSE in serum occurred within 6 h following exposure to either "composite" or primary blast, and persisted up to 7 days post-blast. Average serum UCH-L1 level was also elevated during 1–7 days after "primary" blast (**Figure 5B**), though its difference from controls was statistically significant only at 1 day post-blast.

Glia cell-specific up-regulation of GFAP and CNPase in brain after either "composite" or primary blast was accompanied by a significant serum accumulation of GFAP and CNPase biomarkers measured by SW ELISA for GFAP (**Figure 6A**) and semi-quantitative western blot densitometry for serum CNPase (**Figure 6B**). These biomarkers persisted in blood up to 7 days post-blast at both blast set-ups employed.

SYSTEMIC, VASCULAR INFLAMMATORY, NEUROENDOCRINE AND GROWTH FACTOR RESPONSES FOLLOWING DIFFERENT BLAST EXPOSURES

Based on our previous global and targeted proteomic data, the following molecular components and injury biomarkers were assessed in rat serum. Systemic/vascular responses: interleukin-1 and interleukin-10 (IL-1, IL-10), adipo-chemokine Fractalkine/CX3CL1, Integrin α/β, a complement receptor composed of CD11c/CD18, sICAM-1, and L-, E-selectin.

CYTOKINE/CHEMOKINE LEVELS AFTER BLAST EXPOSURES

We hypothesized that systemic responses and neuroinflammmation together with impaired vascular reaction in the brain, result in enhancement of endothelial permeability/leakage, infiltration of macrophages from circulation and activation of brain-resident microglia cells. As can be seen in **Figures 7A,B**, both pro-inflammatory (IL-1) and counteracting anti-inflammatory molecules (IL-10) accumulate in circulation at 24 h after open body exposure to frontal (off-axis) blast. These results are in agreement with data obtained using non-blast TBI models (Dietrich et al., 2004; Maegele et al., 2007). Moreover, CX3CL1 chemokine Fractalkine was also significantly elevated after primary blast further suggesting a systemic component in response to blast (**Figure 7C**) consistent with reports on the level of this chemokine in patients with TBI and in mouse model of closed head injury (Rancan et al., 2004; Ralay Ranaivo et al., 2011). While immune cell-derived IL-1, IL-10, and fractalkine were significantly increased predominantly after primary blast exposure, integrin alpha/beta levels were elevated at all set-ups indicating that blast is triggering microcirculatory disorders whether it produces head hyperacceleration or not.

SERUM ACCUMULATION OF SICAM-1 AND L-SELECTIN CONNECTING VASCULAR INFLAMMATORY AND TISSUE DAMAGE

Soluble intercellular adhesion molecule, E-selectin and L-selectin are adhesion molecules which reflect the activation of the vascular component of inflammation and interaction of circulatory cells with the endothelial component of blood–brain-barrier (BBB; Nottet, 1999; Whalen et al., 1999, 2000). sICAM levels in serum

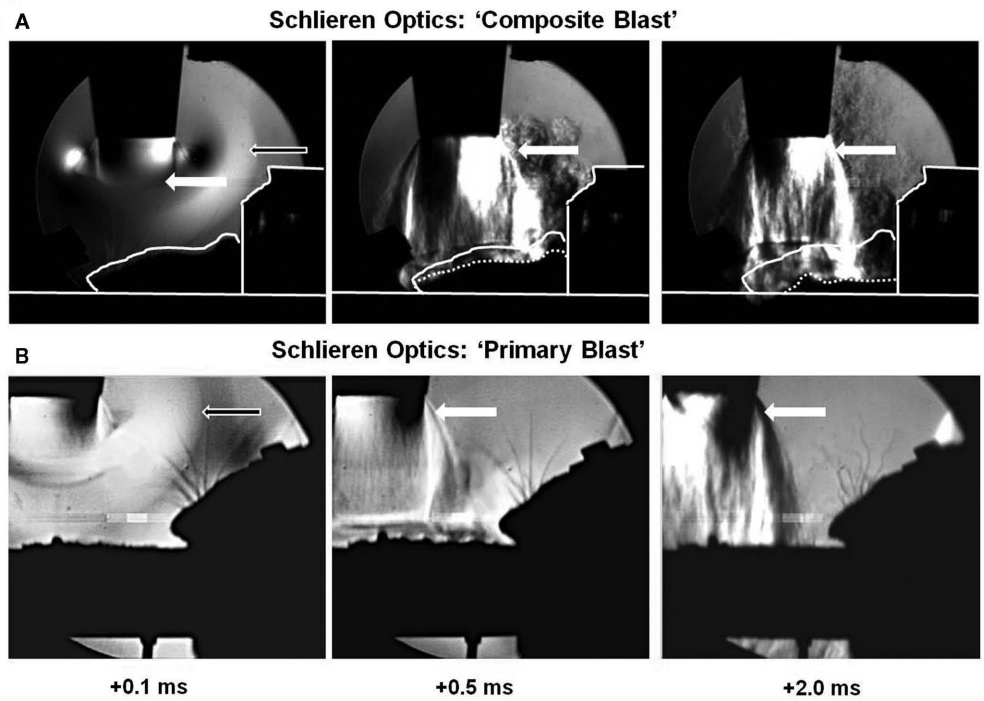

FIGURE 2 | Visualization of blast wave interaction with head on-axis ("composite" blast) and off-axis (primary blast) using Schlieren optics. High speed recording with Schlieren optics: **(A)** "composite blast"; **(B)** "primary blast." Black arrows indicate formation, traveling, and interaction of blast wave with rat head (accomplished within ∼0.1 ms). White arrows show gas venting jet hitting rat head after blast wave passed through (persists for milliseconds). The solid contour line in **(A)** outlines the shape of animal head at time point 0; the dotted line-current shape. Please see Section "Materials and Methods" for details.

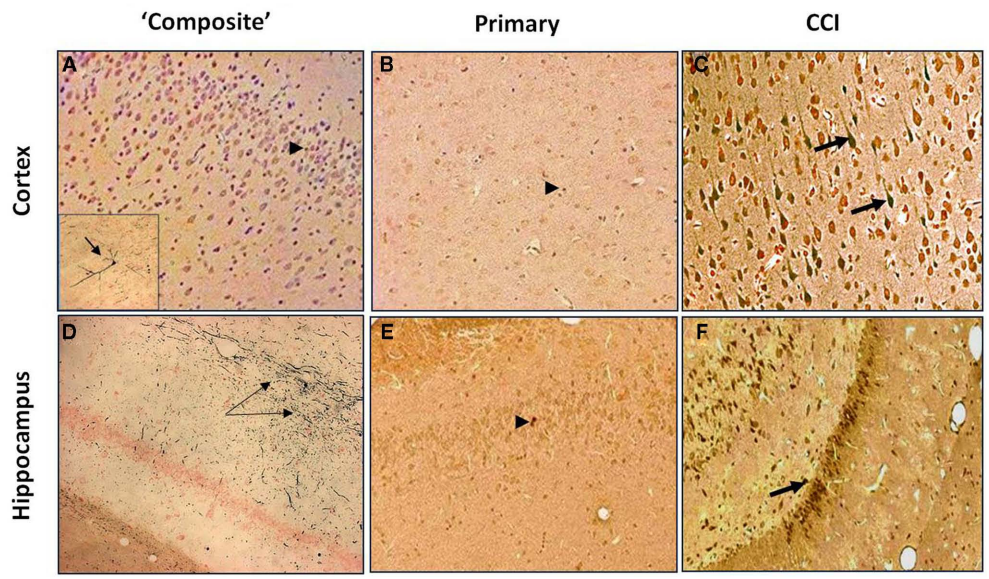

FIGURE 3 | Silver Staining of coronal brain sections following primary or "composite" blast exposure. Corresponding tissue staining 7 days after "composite blast," primary blast, and CCI is shown in **(A–C)** for cortex, and in **(D–F)** for hippocampus. Arrowheads indicate occasional silver accumulation in the cells of non-neuronal origin. Arrows indicate diffuse silver accumulation in neurons. **Figure 3A** inset: a very rare accumulation of silver in a cortical neuron. Please see Section "Materials and Methods" for details.

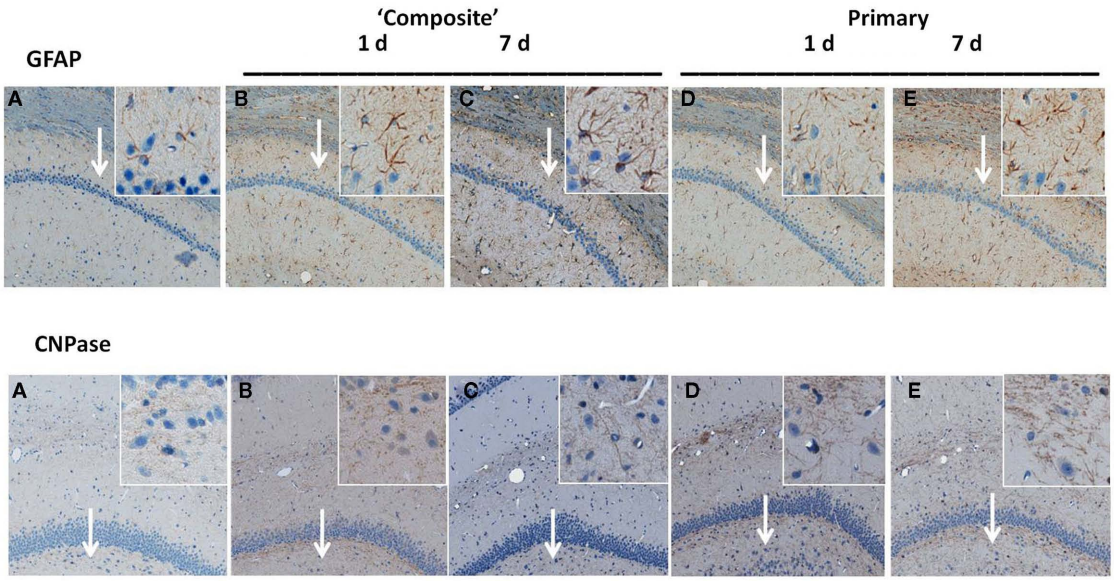

FIGURE 4 | Immunohistochemical analysis of astrocyte and oligodendrocyte markers in hippocampus after blast. Time-dependent GFAP and CNPase expression was studied by IHC on paraffin-embedded 6 μm brain sections after blast exposure at different set-ups. **(A)** Naive; **(B)** "composite" blast, 1 day; **(C)** "composite," 7 days; **(D)** "primary," 1 day; and **(E)** "primary," 7 days. Magnifications 5× and 20× (insets) are shown. Arrows indicate inset locations for CA1 region (GFAP) and DG region (CNPase) in hippocampus. Please see Section "Materials and Methods" for details.

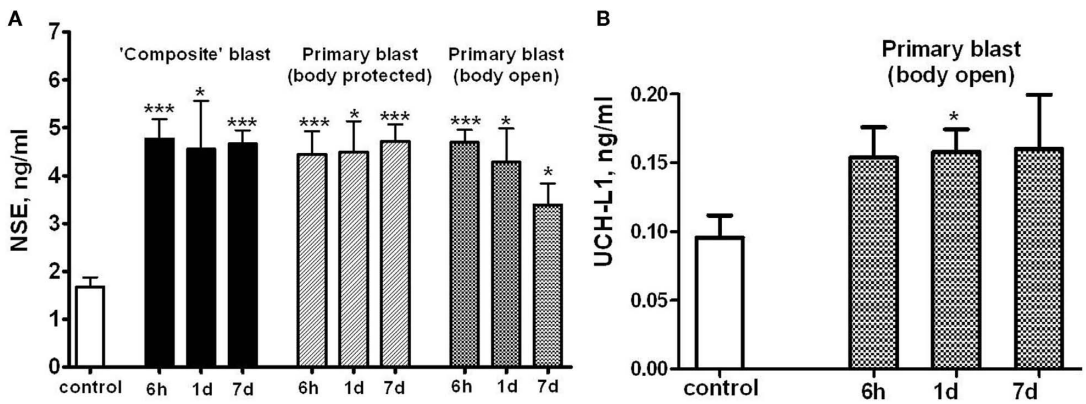

FIGURE 5 | Blast-induced accumulation of NSE and UCHL-1 in rat serum. Blood was collected from overpressure-exposed rats at different shock tube set-ups and assayed by NSE **(A)** and UCHL1 **(B)** SW ELISA Kits. Unpaired *t*-test was used to analyze statistical significance of values. Data shown are mean ± SEM of at least three independent experiments. $*p < 0.05$; $**p < 0.01$; $***p < 0.005$ vs. naïve. Please see Section "Materials and Methods" for details.

raised nearly fourfold within 6 h post-blast, followed by a decline to lower, but still significantly higher than control levels, values at day 7 after exposure to both composite and primary blast (**Figure 8A**). In contrast, serum L-selectin content increased remarkably at 1 and 7 days, but not 6 h following blast (**Figure 8B**). Thus, the prominent activation of the L-selectin component of blast responses occurs when peak overpressure interacts with the frontal part of the head without significant acceleration, reflecting a somewhat delayed involvement of leukocytes compared with earlier (6 h) vascular endothelial activation indicated by sICAM-1 and, to some extent, serum integrin alpha/beta increases.

NEUROENDOCRINE, NEUROTROPHIC, AND GROWTH FACTOR RESPONSES AFTER BLAST EXPOSURE

Orexin A is a neuropeptide secreted by the hypothalamus, which promotes food intake, wakefulness, and metabolic activity/energy consumption. As seen in **Figure 9**, a nearly threefold increase in serum Orexin A occurs 1 and 7 days after primary blast with open body, but not after composite blast, at least within the 7 day interval.

Using a targeted approach, we identified additional components of neurotrophic response to blast exposure – nerve growth factor beta (NGF-beta) and Neuropilin-2 (NRP-2). NGF-beta has

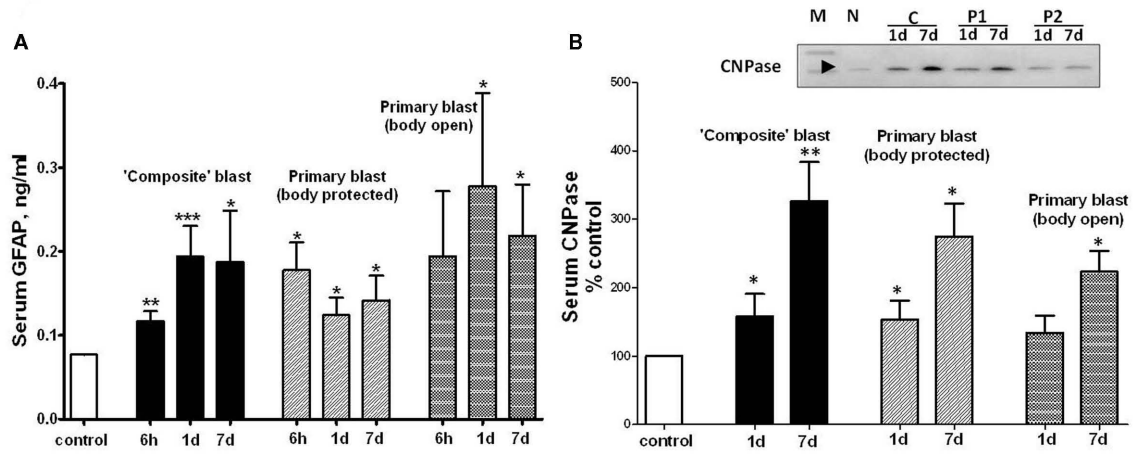

FIGURE 6 | GFAP and CNPase levels in blood after different blast exposures. Blood was collected after OP exposure at different shock tube set-ups. **(A)** Serum GFAP detection by SW ELISA; **(B)** semi-quantitative serum CNPase detection by western blot densitometry. Inset: representative western blot. (N, naïve; C, "composite"; P1, primary/head; P2, primary/body). *t*-Test with Welch correction was done. Data shown are mean ± SEM of at least three independent experiments. $*p < 0.05$; $**p < 0.01$; $***p < 0.005$ vs. naïve. Please see Section "Materials and Methods" for details.

been suggested to play a neurotrophic role in several neurodegenerative diseases (Li et al., 2007; Syed et al., 2007; Calissano et al., 2010). Neuropilin-2 is a receptor for VEGF and semaphorins, a large family of secreted and transmembrane signaling proteins that regulate axonal guidance in the developing CNS (Cloutier et al., 2002; Bannerman et al., 2008; Roffers-Agarwal and Gammill, 2009). Serum levels of NGF-beta were assessed using SW ELISA and NRP-2 by antibody array (Ray Biotech) and semi-quantitative western blot after blast exposure at different set-ups (**Figure 10**). Generally, exposures to composite and primary blast resulted in a significant increase of NGF-beta in serum 1 and 7 day after challenge, however the magnitude of increase was much higher after primary blast hit open body compared to composite blast exposure (**Figure 10A**). Likewise, high levels of NRP-2 were found in circulation at 1 and 7 day in rats exposed to primary blast with unprotected body, as compared to composite blast together with NRP-2 up-regulation in hippocampus at all blast set-ups. These data suggest that predominantly primary blast activates neuroregeneration and that NRP-2 may be involved in this process. In addition, these results indicate that NGF-beta and NRP-2 may have neuroprotective functions and be involved in adaptive responses/neurorepair after blast-induced TBI.

DISCUSSION

Over the last several decades, a number of experimental animal models to study blast wave effects have been implemented, including rodents and larger animals, such as sheep (Savic et al., 1991; Stuhmiller et al., 1996). Shock tubes have been used as the fundamental research tool for the last several decades (Jaffin et al., 1987; Elsayed, 1997; Guy et al., 1998a,b). There is still concern whether a blast waves generated by shock tubes using compressed gas accurately reflect real explosive blast. In our study, dynamic pressure measured by a PCB "pencil" sensor indicated that shock tubes produce a "venting gas jet" immediately after blast wave formation (see the shoulder at **Figure 1A**), substantially contaminating the blast wave in the direction of shock tube axis (**Figure 1A**). In addition, the exhaust "venting gas" apparently masked the negative phase of the shock wave, which was present when the dynamic pressure was recorded at an angle to the shock tube nozzle (**Figure 1B**). Schlieren optics techniques clearly defined the areas of pressure, either peak OP or venting gas jet (**Figure 2**).

This pattern is characteristic of "external" shock tube models where the target/animal is placed outside rather than within the tube. Placing animals within the tube also can produce confounding effects when the animal is very large relative to the tube diameter or when the animal is suspended and or shielded inappropriately. The shape of the blast wave and the development of constructive or destructive secondary waves as the primary wave exits the tube can be affected by the size and shape of the exit as well. This can be visualized with Schlieren optics. By placing rats off-axis from the shock tube nozzle, we eliminated the venting gas in a way that the main effect acting on the rat is the peak overpressure event and negative phase of the blast wave. Thus, we examined the pathological impact of two different types of blast with precisely controlled magnitude, duration, and impulse at the surface of the rat, different orientations of the head to the blast wave, and open or armored body: (i) primary blast/peak overpressure only with rats located off-axis with the shock tube and (ii) composite blast with rats located on-axis, accompanied by linear and, to a lesser extent, rotational head hyperacceleration (**Figure 2**). It should be noted that any blast produced in the laboratory models only a particular component of a complex blast that might be experienced on the battlefield. The detonation of real explosives in the field does not produce the "venting gas," but can result in significant bulk flow of air and debris. This makes the separation of the effects of primary and particularly tertiary blast (the target being displaced by the blast) difficult to separate in most existing testing regimes. Although the blast generated in our on-axis model is a single blast event, the type of blast load observed resembles the complex effect produced by multiple blasts, such as in a confined

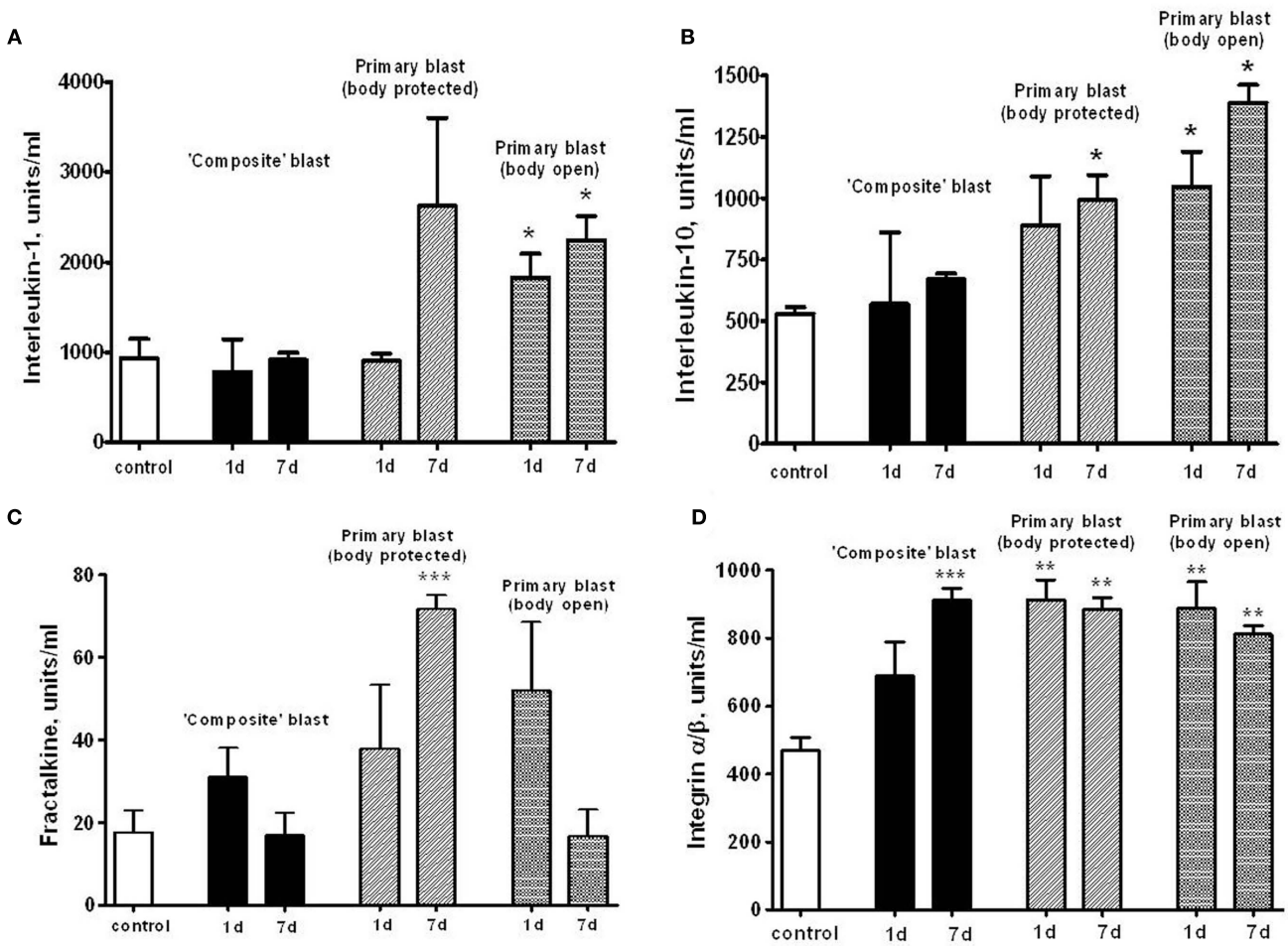

FIGURE 7 | Serum levels of interleukins, fractalkine, and integrin α/β after blast. Concentrations of interleukin-1 **(A)**, interleukin-10 **(B)**, fractalkine **(C),** and integrin α/β **(D)** were assessed in rat serum by RayBiotech antibody arrays. Please see Section "Materials and Methods" for details. Blood was collected from OP-exposed rats at different shock tube set-ups. Unpaired *t*-test was used to analyze statistical significance of values. Data shown are mean ± SEM of at least three independent experiments. $*p < 0.05$; $**p < 0.01$; $***p < 0.005$.

space where the blast waves reverberate and overlap, hence the effect of displaced air mass flow on the resultant wave structure and magnitude can be important.

There was a substantial difference in the effects of composite vs. primary blast on neurodegenerative processes in the cortex and, particularly, hippocampus at 7 day post-blast (**Figure 3**). Silver accumulation in the cortex after composite blast was modest, with a very rare finding of "classical type" neurodegeneration (**Figure 3A**, inset). On the other hand, the hippocampus significantly accumulated silver in fiber-like structures after composite blast (**Figure 3D**), while very occasional silver staining was observed in both cortex and hippocampus after primary blast (**Figures 3B,E**). As expected and in accordance with data reported previously, CCI evoked a distinct cellular neurodegeneration in both cortical and hippocampal tissue (**Figures 3C,F**). The most common types of closed head impact TBI are diffuse axonal injury, contusion, and subdural hemorrhage as an overall result of rotational acceleration (Vander Vorst et al., 2007). Diffuse axonal injuries are very common following closed head injuries. They result when shearing, stretching, and/or angular forces pull on axons and small vessels. Impaired axonal transport leads to focal axonal swelling and, after several hours, may result in axonal disconnection (Hurley et al., 2004). The typical locations are the corticomedullary (gray matter-white matter) junction, internal capsule, deep gray matter, upper brainstem, and corpus callosum. Multifocal axonal degeneration, as evidenced by amino cupric silver staining is characteristic also for shock wave insult as was shown in a study with head-only exposed rats inside a shock tube (Garman et al., 2011). Our recent (Svetlov et al., 2010) and present studies clearly demonstrate the presence of neural degeneration in deeper structures of the brain, specifically hippocampus after composite blast producing linear and rotational head acceleration, which is lacking or negligible following primary blast.

Exposure to a single moderate blast, both composite and primary, led to prominent gliosis in the hippocampus, evidenced by expression of GFAP and CNPase (**Figure 4**). Markers of activated

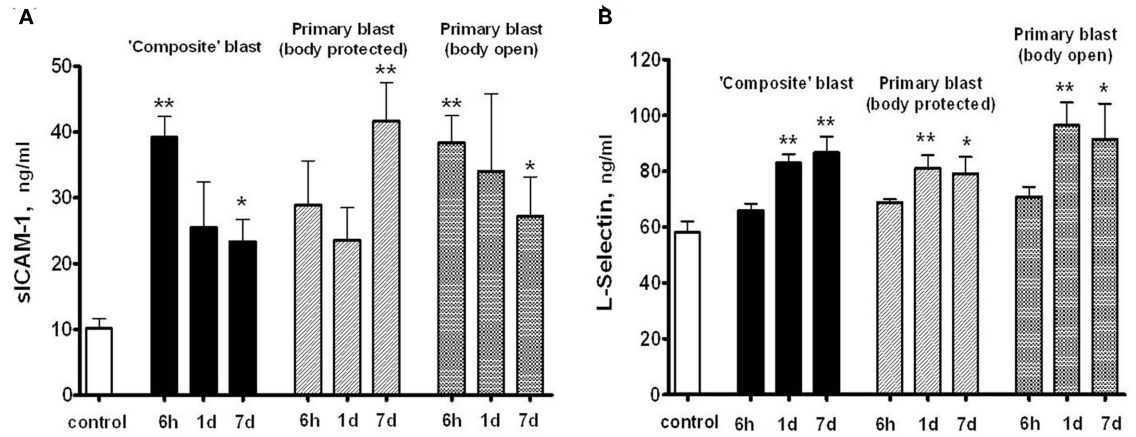

FIGURE 8 | Soluble intercellular adhesion molecule -1 (A) and L-selectin (B) concentrations in rat serum following blast exposure. Blood was collected after blast at different shock tube set-ups and assayed by SW ELISA. Unpaired *t*-test was done to analyze statistical significance of values. Data shown are mean ± SEM of at least three independent experiments. $*p < 0.05$; $**p < 0.01$; $***p < 0.005$ vs. naïve. Please see Section "Materials and Methods" for details.

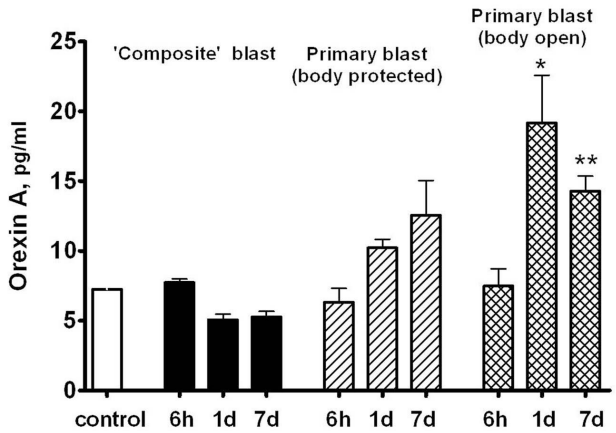

FIGURE 9 | Orexin A content in rat serum after blast. Blood was collected from overpressure-exposed rats at different shock tube set-ups and assayed by SW ELISA. Unpaired *t*-test was done to analyze statistical significance of values. Data shown are mean ± SEM of at least three independent experiments. $*p < 0.05$; $**p < 0.01$; $***p < 0.005$ vs. naïve. Please see Section "Materials and Methods" for details.

astrocytes GFAP and oligodendrocytes CNPase were strongly up-regulated in CA1 and DG regions of hippocampus, respectively, at 1 day and sustained up to 7 days post-blast. These findings are in strict accordance with many previous reports, including from our group, supporting the notion that gliosis represents a common and rapid response to brain insult regardless of the nature-mechanical or blast-induced exposure (Urrea et al., 2007; Svetlov et al., 2010; Kwon et al., 2011).

NSE was significantly elevated in serum within 6 h after both composite and primary blast (**Figure 5A**), and the increased levels generally persisted up to 7 days, although was not statistically significant upon open body primary blast exposure. In these experiments, we used NSE SW ELISA Kit from Life Sciences Advanced Technologies designed to detect specifically rat NSE. However, several reports indicate that NSE may not be highly specific for the CNS and is present in platelets and red blood cells (see Svetlov et al., 2009 for review). In previous studies, we reported a slight UCH-L1 increase after "composite" blast, followed by a rapid decline (Svetlov et al., 2010). The UCH-L1 SW ELISA used in early experiments had low specificity and sensitivity for rat samples, thus many serum substances interfered and masked the UCH-L1 content. In this study, an improved version of the UCH-L1 assay was employed, still not particularly specific for rats (data not shown). Increases in serum UCH-L1 were statistically significant only at day 1 after a single primary blast exposure ($n = 4$), although an elevation trend could be detected (**Figure 5B**). In contrast, a rat-specific GFAP SW ELISA has been generated and employed in these studies. Serum GFAP increase was prominent within 6 h after composite and primary blast with body protected (**Figure 6A**), and elevated levels persisted up to 7 days post-blast, consistent with up-regulation in hippocampus. The CNPase content assessed by semi-quantitative western blot was raised at day 1 after blast exposure (except primary blast with open body) and further substantially increased at 7 day post-blast (**Figure 6B**). It remains to be examined whether CNPase up-regulation reflects a long-term disorder of myelination following blast exposure and whether CNPase can be a biomarker of chronic injury.

We postulated that impaired vascular reactions, systemic responses, and neuroinflammmation, result in enhancement of endothelial permeability/leakage, recruitment of immune/inflammatory cells from circulation, and activation of brain-resident glial cells. This paradigm is in line with the previous hypothesis set forth by Cernak (2010) and is further supported by present data.

As can be seen in **Figures 7A,B**, both pro-inflammatory (IL-1) and counteracting anti-inflammatory molecules (IL-10) accumulate in circulation at 1 and 7 days post-blast, predominantly after

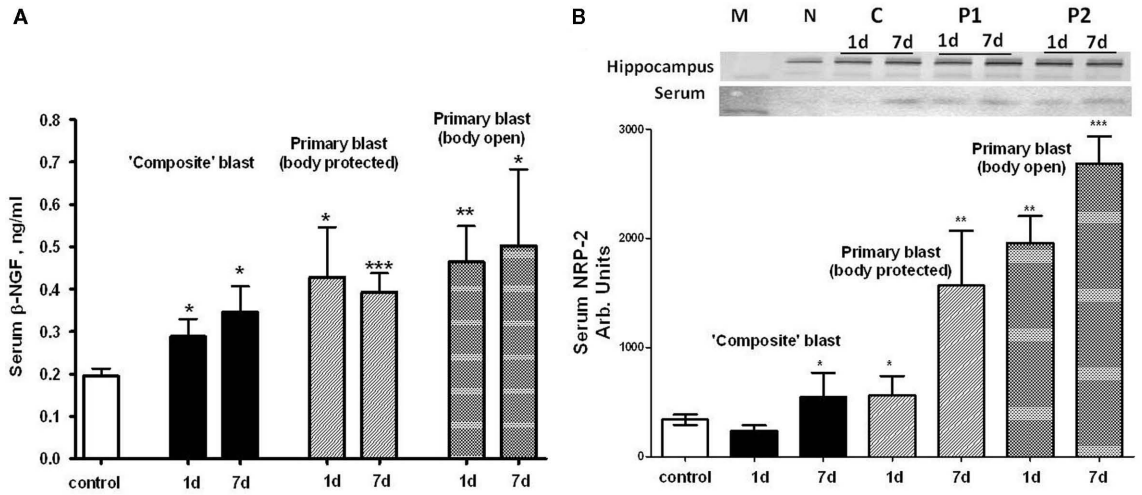

FIGURE 10 | Blast-induced accumulation of β-NGF and Neuropilin-2 in rat serum. (A) Serum β-NGF after different types of blast (SW ELISA); **(B)** serum Neuropilin-2 detection by antibody arrays. Inset: representative western blots for hippocampus and serum. (N, naïve; C, "composite"; P1, primary/head; P2, primary/body). *t*-Test with Welch correction was done. Data shown are mean ± SEM of at least three independent experiments. $*p < 0.05$; $**p < 0.01$; $***p < 0.005$ vs. naïve. Please see Section "Materials and Methods" for details.

primary blast exposure with open body (**Figures 7A,B**). These results are in agreement with data obtained using non-blast TBI models (Dietrich et al., 2004; Maegele et al., 2007). Moreover, CX3CL1 chemokine Fractalkine was also significantly elevated after primary blast (mostly with protected body), further suggesting a systemic component in response to blast (**Figure 7C**), consistent with reports on the level of this chemokine in patients with TBI and in mouse model of closed head injury (Rancan et al., 2004; Ralay Ranaivo et al., 2011). Most intriguing is that serum IL-1, IL-10, and Fractalkine did not rise significantly after composite blast at 1 and 7 days post-blast. In contrast, integrin alpha/beta, a complement receptor composed of CD11c/CD18, was increased substantially at all set-ups (**Figure 7D**), further supporting the important roles for a microcirculatory component of neuroinflammation in brain injury shown in rat models of fluid percussion injury (Utagawa et al., 2008).

L-selectin and ICAM-1 are adhesion molecules which characterize the activation of a vascular component of inflammation and interaction of circulatory cells with the endothelial component of the (BBB; Nottet, 1999; Whalen et al., 1999, 2000). As can be seen in **Figure 8**, prominent activation of the L-selectin after blast occurs when peak overpressure interacts with the frontal part of head without significant acceleration, reflecting a somewhat delayed involvement of leukocytes compared with earlier (6 h) vascular endothelial activation reflected by sICAM-1 and, to some extent, serum integrin alpha/beta increases. Thus, the sustained activation of vascular components of blast responses occurs when peak overpressure interacts with the frontal part of the head without significant acceleration: "flowing blast inside the brain" (blast off-axis open body).

Orexin A, a neuroendocrine component of rat response to blast exposure, exhibited the most prominent pattern of difference between composite and primary blast (**Figure 9**). Serum Orexin A levels raised gradually within 1–7 days after primary blast and were significantly elevated in rats subjected to blast with open body. Although at present the precise mechanisms are not clear, this suggests that several systemic factors affected by primary blast wave in the whole body other than brain structures directly or indirectly stimulate hypothalamic release of Orexin A as well as interleukins/chemokines in circulation. We speculate that the presence of a distinct negative phase in primary blast wave is capable of producing cavitation-induced secondary microblasts. This could partially explain the different pattern in systemic/vascular responses to primary vs. composite blast exposure which lacks the negative phase. Further in-depth studies are needed to explore this hypothesis and elucidate potential roles for blast cavitation in damage, particularly at the interface of gas, liquid, and tissue.

Beta-NGF has been suggested to play a neurotrophic role in several neurodegenerative diseases (Li et al., 2007; Syed et al., 2007; Calissano et al., 2010). Our data indicate that NGF may also have neuroprotective functions and be involved in adaptive responses/neurorepair after blast-induced TBI. Exposure of whole body to primary overpressure blast instigated a rapid and sustained accumulation of beta-NGF in serum. Neuropilin-2 is the receptor for VEGF and semaphorins, a large family of secreted and transmembrane signaling proteins that regulate axonal guidance in the developing CNS (Cloutier et al., 2002; Bannerman et al., 2008; Roffers-Agarwal and Gammill, 2009). Our present data (**Figure 10B**) suggest that predominantly primary blast activates neuroregeneration and that NRP-2 may be involved in this process.

In conclusion, the specific dynamics of systemic, vascular inflammatory, neuroendocrine, growth factor, and neuroglial biomarkers in serum were established and characterized. For major pathway signatures and biomarkers, the detected levels raised at all the set-ups studied. However, the most

significant and persistent changes in neuro-glial injury markers were found after composite blast, while primary blast instigated the most prominent systemic/vascular, neuroendocrine, and growth factor responses, particularly when the rat was subjected to frontal, head-directed, open body exposure. We suggest that the mechanisms underlying primary blast brain injuries, particularly mild and moderate, are different from blast accompanied by head acceleration and may be triggered by systemic, cerebrovascular, and neuro-glia responses as overlapping events.

ACKNOWLEDGMENTS

The authors wish to thank Mr. Danny Johnson for his excellent technical assistance. This work was supported by grants W81XWH-8-1-0376 and W81XWH-07-01-0701 from Department of Defense. The research was conducted in the absence of any commercial or financial relationships that could be construed as a potential conflict of interest. The views and opinions expressed in this manuscript are those of the author(s) and do not reflect official policy or position of the Department of Defense or the U.S. Government.

REFERENCES

Bannerman, P., Ara, J., Hahn, A., Hong, L., McCauley, E., Friesen, K., and Pleasure, D. (2008). Peripheral nerve regeneration is delayed in neuropilin 2-deficient mice. *J. Neurosci. Res.* 86, 3163–3169.

Bass, C. R., Panzer, M. B., Rafaels, K. A., Wood, G., Shridharani, J., and Capehart, B. (2012). Brain injuries from blast. *Ann. Biomed. Eng.* 40, 185–202.

Belanger, H. G., Scott, S. G., Scholten, J., Curtiss, G., and Vanderploeg, R. D. (2005). Utility of mechanism-of-injury-based assessment and treatment: Blast Injury Program case illustration. *J. Rehabil. Res. Dev.* 42, 403–412.

Born, C. T. (2005). Blast trauma: the fourth weapon of mass destruction. *Scand. J. Surg.* 94, 279–285.

Calissano, P., and Matrone, C., Amadoro, G. (2010). Nerve growth factor as a paradigm of neurotrophins related to Alzheimer's disease. *Dev. Neurobiol.* 70, 372–383.

Cernak, I. (2010). The importance of systemic response in the pathobiology of blast-induced neurotrauma. *Front. Neurol.* 1:151. doi:10.3389/fneur.2010.00151

Cernak, I., Merkle, A. C., Koliatsos, V. E., Bilik, J. M., Luong, Q. T., Mahota, T. M., Xu, L., Slack, N., Windle, D., and Ahmed, F. A. (2011). The pathobiology of blast injuries and blast-induced neurotrauma as identified using a new experimental model of injury in mice. *Neurobiol. Dis.* 41, 538–551.

Cernak, I., and Noble-Haeusslein, L. J. (2010). Traumatic brain injury: an overview of pathobiology with emphasis on military populations. *J. Cereb. Blood Flow Metab.* 30, 255–266.

Cernak, I., Savic, J., Ignjatovic, D., and Jevtic, M. (1999). Blast injury from explosive munitions. *J. Trauma.* 47, 96–103; discussion 103–104.

Chavko, M., Adeeb, S., Ahlers, S. T., and McCarron, R. M. (2009). Attenuation of pulmonary inflammation after exposure to blast overpressure by N-acetylcysteine amide. *Shock* 32, 325–331.

Cloutier, J. F., Giger, R. J., Koentges, G., Dulac, C., Kolodkin, A. L., and Ginty, D. D. (2002). Neuropilin-2 mediates axonal fasciculation, zonal segregation, but not axonal convergence, of primary accessory olfactory neurons. *Neuron* 33, 877–892.

Dietrich, W. D., Chatzipanteli, K., Vitarbo, E., Wada, K., and Kinoshita, K. (2004). The role of inflammatory processes in the pathophysiology and treatment of brain and spinal cord trauma. *Acta Neurochir. Suppl.* 89, 69–74.

Elsayed, N. M. (1997). Toxicology of blast overpressure. *Toxicology* 121, 1–15.

Garman, R. H., Jenkins, L. W., Switzer, R. C., Bauman, R. A., Tong, L. C., Swauger, P. W., Parks, S. A., Ritzel, D. V., Dixon, C. E., Clark, R. S. B., Bayir, H., Kagan, V., Jackson, E. K., and Kochanek, P. M. (2011). Blast exposure in rats with body shielding is characterized primarily by diffuse axonal injury. *J. Neurotrauma* 28, 947–959.

Guy, R. J., Glover, M. A., and Cripps, N. P. (1998a). The pathophysiology of primary blast injury and its implications for treatment. Part I: the thorax. *J. R. Nav. Med. Serv.* 84, 79–86.

Guy, R. J., Kirkman, E., Watkins, P. E., and Cooper, G. J. (1998b). Physiologic responses to primary blast. *J. Trauma.* 45, 983–987.

Gyorgy, A., Ling, G., Wingo, D., Walker, J., Tong, L., Parks, S., Januszkiewicz, A., Baumann, R., and Agoston, D. V. (2011). Time-dependent changes in serum biomarker levels after blast traumatic brain injury. *J. Neurotrauma* 28, 1121–1126.

Hurley, R. A., McGowan, J. C., Arfanakis, K., Taber, K. H. (2004). Traumatic axonal injury: novel insights into evolution and identification. *J. Neuropsychiatry Clin. Neurosci.* 16, 1–7.

Jaffin, J. H., McKinney, L., Kinney, R. C., Cunningham, J. A., Moritz, D. M., Kraimer, J. M., Graeber, G. M., Moe, J. B., Salander, J. M., and Harmon, J. W. (1987). A laboratory model for studying blast overpressure injury. *J. Trauma.* 27, 349–356.

Jones, E., Fear, N. T., and Wessely, S. (2007). Shell shock and mild traumatic brain injury: a historical review. *Am. J. Psychiatry* 164, 1641–1645.

Kinney, G. F. (1985). *Explosive Shocks in Air*. New York: Spinger-Verlag.

Kwon, S. K., Kovesdi, E., Gyorgy, A. B., Wingo, D., Kamnaksh, A., Walker, J., Long, J. B., and Agoston, D. V. (2011). Stress and traumatic brain injury: a behavioral, proteomics, and histological study. *Front. Neurol.* 2:12. doi:10.3389/fneur.2011.00012

Li, Y., Zhang, S. F., Zou, S. E., Xia, X., Bao, L. (2007). Accumulation of nerve growth factor and its receptors in the uterus and dorsal root ganglia in a mouse model of adenomyosis. *Reprod. Biol. Endocrinol.* 9, 30.

Liu, M. C., Akinyi, L., Scharf, D., Mo, J., Larner, S. F., Muller, U., Oli, M. W., Zheng, W., Kobeissy, F., Papa, L., Lu, X. C., Dave, J. R., Tortella, F. C., Hayes, R. L., and Wang, K. K. (2010). Ubiquitin C-terminal hydrolase-L1 as a biomarker for ischemic and traumatic brain injury in rats. *Eur. J. Neurosci.* 31, 722–732.

Maegele, M., Sauerland, S., Bouillon, B., Schafer, U., Trubel, H., Riess, P., and Neugebauer, E. A. (2007). Differential immunoresponses following experimental traumatic brain injury, bone fracture and "two-hit"-combined neurotrauma. *Inflamm. Res.* 56, 318–323.

Nelson, T. J., Wall, D. B., Stedje-Larsen, E. T., Clark, R. T., Chambers, L. W., and Bohman, H. R. (2006). Predictors of mortality in close proximity blast injuries during Operation Iraqi Freedom. *J. Am. Coll. Surg.* 202, 418–422.

Nottet, H. S. (1999). Interactions between macrophages and brain microvascular endothelial cells: role in pathogenesis of HIV-1 infection and blood – brain barrier function. *J. Neurovirol.* 5, 659–669.

Ralay Ranaivo, H., Zunich, S., Choi, N., Hodge, J., Wainwright, M. (2011). Mild stretch-induced injury increases susceptibility to interleukin-1beta-induced release of matrix metalloproteinase-9 from astrocytes. *J Neurotrauma.* 28, 1757–1766.

Rancan, M., Bye, N., Otto, V. I., Trentz, O., Kossmann, T., Frentzel, S., and Morganti-Kossmann, M. C. (2004). The chemokine fractalkine in patients with severe traumatic brain injury and a mouse model of closed head injury. *J. Cereb. Blood Flow Metab.* 24, 1110–1118.

Roffers-Agarwal, J., and Gammill, L. S. (2009). Neuropilin receptors guide distinct phases of sensory and motor neuronal segmentation. *Development* 136, 1879–1888.

Savic, J., Tatic, V., Ignjatovic, D., Mrda, V., Erdeljan, D., Cernak, I., Vujnov, S., Simovic, M., Andelic, G., and Duknic, M. (1991). Pathophysiologic reactions in sheep to blast waves from detonation of aerosol explosives. *Vojnosanit. Pregl.* 48, 499–506.

Stuhmiller, J. H., Ho, K. H., Vander Vorst, M. J., Dodd, K. T., Fitzpatrick, T., and Mayorga, M. (1996). A model of blast overpressure injury to the lung. *J. Biomech.* 29, 227–234.

Svetlov, S. I, Prima, V., Kirk, D. R., Gutierrez, H., Curley, K. C., Hayes, R. L., and Wang, K. K. W. (2011). "Neuro-glial and systemic mechanisms of pathological responses to primary blast overpressure (OP) compared to "composite" blast accompanied by head acceleration in rats," in Proceeding of NATO conference 'A Survey of Blast Injury across the Full Landscape of Military Science http://www.rto.nato.int/

Svetlov, S. I., Larner, S. F., Kirk, D. R., Atkinson, J., Hayes, R. L., and Wang, K. K. (2009). Biomarkers of blast-induced neurotrauma: profiling molecular and cellular mechanisms of blast brain injury. *J. Neurotrauma* 26, 913–921.

Svetlov, S. I., Prima, V., Kirk, D. R., Gutierrez, H., Curley, K. C., Hayes,

MULTIPLE BLAST EXPOSURES ALTERS NEURO-GLIAL, NEUROENDOCRINE AND GROWTH FACTOR BIOMARKERS TO BLAST LOAD IN RATS

Prima V[1] , Scharf D[1], Gutierrez H[2], Kirk DR[2] Svetlov A[1], Curley KC[3], Hayes RL[1], Svetlov SI[1]

[1]Banyan Biomarkers; [2]Florida Institute of Technology; [3]US Army Medical Research and Material Command

Abstract

PROBLEM/CHALLENGE: Blast-induced neurotrauma is frequently accompanied by blood–brain barrier (BBB) disruption, which permits the release of brain-specific proteins into circulation and facilitates exchange of neuromediators. While repeated blast exposures is a common hazard for war zone personnel and civilian populations, the cumulative effects of multiple blasts on brain injury biomarkers have not been investigated.

PURPOSE: Evaluate the potential cumulative effects of blast load by comparing the responses after multiple blast exposures to a single overpressure event, inducing brain injury in rats.

DESIGN: Rats were subjected to a primary blast of 365 kPa overpressure and total duration of 75 μsec at the frontal part of the rat's skull. Portable cumulative blast sensors were placed on the head front and rat spine. Multiple blasts were performed as a series of 3 exposures, with a 45 min to 1 hr recovery period between each blast. High speed imaging revealed a negligible degree of acceleration at rat position "off-axis" toward external shock tube, thus confirming primary blast kinematics.

METHODS: Assessment of previously characterized and potential novel TBI biomarkers was done by ELISA, antibody microarrays, and Western blot. We measured blood accumulation of glial markers (GFAP and CNPase), neuronal markers (UCH-L1 and NSE), neuroendocrine peptide Orexin A, and Neuropilin-2 (receptor for VEGF and semaphorins) at 1 day and 7 days post-blast.

RESULTS: Remarkable elevation of all proteins studied was observed at 1 day after either single or multiple exposures to blast. Of note, multiple blasts significantly increased blood levels of GFAP, UCH-L1, NSE and NRP-2, but not Orexin A, vs. single blast exposure 1 day post-blast, while at 7 days the cumulative effects of multiple blasts were much lower, if any, compared to a single blast. On the other hand, serum CNPase after multiple blasts was significantly elevated compared to single blast both at 1 day and 7 days post exposure.

Summary: The time-course of several serum biomarkers of neurotrauma was characterized after single and repeated moderate primary blasts. Biomarker levels rose significantly as a rapid response at day one post-blast, with the CNPase, NSE, UCH-L1, and NRP-2 levels after repeated blast exposures elevating further over single blast. The appearance of characteristic proteins in circulation may reflect deterioration of the BBB and can be used for assessment of injury accumulation. However, triple consecutive blast exposures did not produce a further elevation in biomarkers at 7 days post exposure compared to a single blast. At this time point, their increased levels depend on the cell-specific origin of biomarkers and that stage of injury, rather than reflecting a cumulative blast load.

Conclusions

- Controlled repeated blast loads in a shock tube animal model were employed to characterize the accumulation of serum biomarkers of neuro-glial injury.
- The high speed imaging revealed that placing rats outside shock tube axis exposed rats to a peak overpressure only (primary blast event), allowing close mimicking of explosive blast TBI and avoiding strong head acceleration/jolting due to the compressed air jet .
- Blood levels rose significantly for GFAP, CNPase, NSE, UCH-L1, Orexin , sICAM and NRP-2. Aas a rapid response at day one post-blast, after repeated blast exposures elevating further over single blast.
- Only for CNPase and sICAM the corresponding systemic levels continued to significantly increase at 7 days post-blast over the 1 day post-blast values.
- For all putative brain-specific biomarkers the serum levels raised substantially at 1 day after multiple blasts however accumulation was not linearly proportional to the number of blasts.
- The above phenomenon was observed also for the leakage of albumin-EBD complex in the reverse direction from circulation to the brain tissue.

Modeling Multiple Blast Exposures

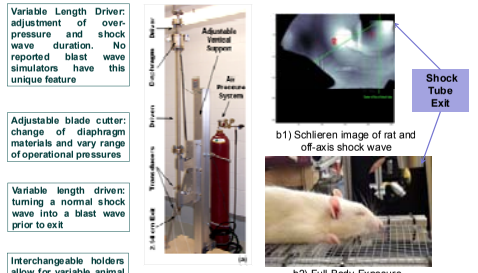

a) Shock Wave Generator setup. b) Animal positioning for the off-axis primary blast. b1) Schlieren imaging. b2) Blast exposure.

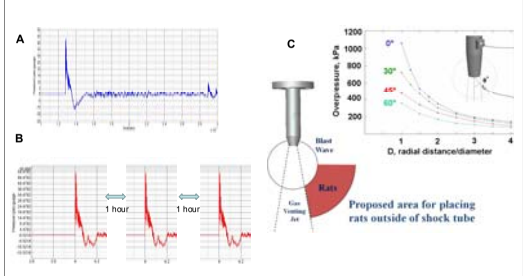

Representative overpressure traces during single (A) and multiple (B) blast exposures; (C) Blast wave overpressure as a function of radial distance and angle.

Neural-Glial TBI Markers released in Blood after Single/Multiple Blast

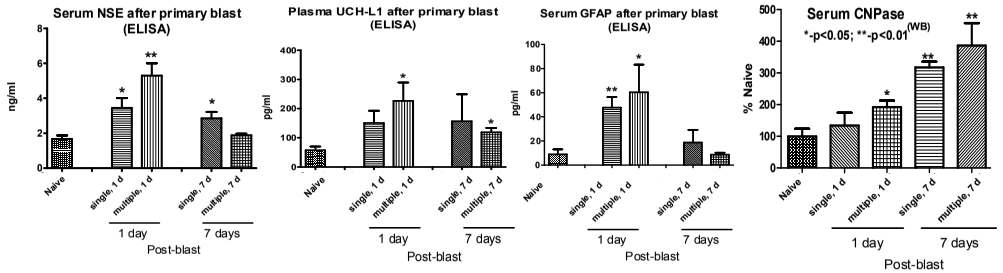

Neuroendocrine, inflammatory and growth factor TBI Markers

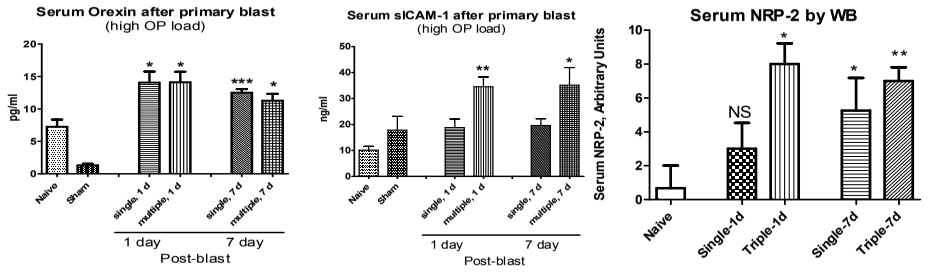

High-Speed Blast Imaging

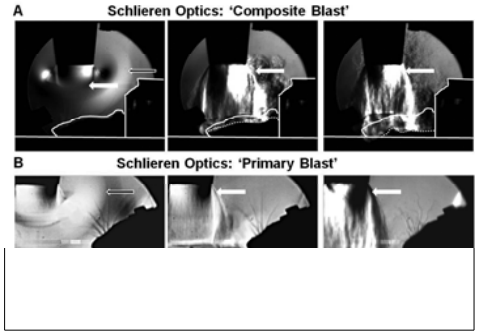

Comparison of blast wave interaction with head On-axis ('Composite' Blast) vs. Off-axis (Primary Blast)

High-speed recording with Schlieren Optics: A) 'Composite Blast'; B) 'Primary Blast'. Black arrows indicate formation and interaction of blast wave with rat head (accomplished within ~0.1 ms). White arrows show gas venting jet hitting rat head after blast wave passed through (persists for milliseconds). The solid contour line in panel A outlines the shape of animal head at time point 0; the dotted line- current shape.

BBB Permeability after Blast

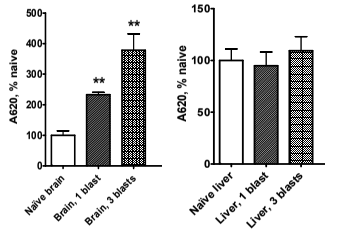

A 2% solution of Evans Blue Dye in PBS (4 mL/kg of body weight) was injected i.p. and the stain was allowed to circulate for 3 hours. At 4 hrs after first blast the anesthetized animals were intracardially perfused with PBS. Brain and liver samples were then isolated and weighed, homogenized in 2 ml 50% trichloroacetic acid per gram tissue and centrifuged. The absorbance of the extracted dye in supernatant at 620 nm was used to quantify the relative tissue content of EBD.

Download this poster

Supported by grants N14-06-1-1029, W81XWH-8-1-0376 and W81XWH-07-01-0701 from Department of Defense.

Neuro-glial and systemic mechanisms of pathological responses to primary blast overpressure (OP) compared to 'composite' blast accompanied by head acceleration in rats.

Stanislav I. Svetlov[1], Victor Prima[1], Daniel R. Kirk[2], Hector Gutierrez[2], Kenneth C. Curley[3], Ronald L Hayes[1], Kevin K.W. Wang[1]

[1]Center of Innovative Research, Banyan Biomarkers Inc., 12085 Research Drive, Alachua, FL 32615, USA

[2]Mechanical & Aerospace Engineering, Florida Institute of Technology, Melbourne FL 32901, USA

[3]U.S. Army Medical Research and Materiel Command, Fort Detrick, Frederick, MD, USA

ssvetlov@banyanbio.com

Energy distribution in modern technosphera, and particularly the 21st century warfare, has led to a significant increase of human exposure to blast overpressure (OP) impulses. Blast forces, even of low magnitude, are believed to produce minor but sustained neurological deficits, and when repeated, can lead to neuro-somatic damage and neurodegeneration. Most prominent changes may occur at the level of intercellular circuits that involve neurons, glia, vascular cells and neural progenitors.

Reproducible models of military-relevant blast injury, including generators which precisely control parameters of the blast wave have been developed and examined. Our studies demonstrated the importance of positional orientation of head and whole body toward blast wave in animal models. Here, we compare the effects of body/head exposure to a moderate primary overpressure (OP) with brain injury produced by a severe blast accompanied by strong head acceleration.

The high speed imaging demonstrated the interaction of blast wave with animal head/body and revealed a negligible degree of acceleration at rat positioning 'off-axis' toward shock tube (primary blast) compared to 'on-axis' experimental setup accompanied by strong head/cervical acceleration. We examined brain expression of glial and neural markers including GFAP and revealed strong glyosis accompanied by a time-dependent proliferation of activated astrocyte and oligodendrocyte lineages after exposures to primary and 'composite' blast. GFAP and neuronal markers UCH-L1 and NSE were also detectable in plasma/serum after blast exposures. Serum levels of IL-1 and IL-10 were significantly elevated, predominantly after primary blast exposure reflecting systemic body responses. Brain up-regulation of cell adhesion molecules L- and E-selectins, nerve growth factor beta-NGF and neuronal receptor Neuropilin-2 was also detected.

A specific dynamics of corresponding biomarkers in serum was established and characterized. For major pathway's signatures and biomarkers, the detected levels raised at all the setups studied. However, the most significant and persistent changes in neuro-glial markers were found after composite blast, while primary blast instigated prominent systemic/vascular reactions, particularly when the total animal body was subjected to blast wave.

In conclusion, several crucial pathogenic components of neural and systemic responses were raised in a time-dependent and setup-dependent fashion. We suggest that the mechanisms underlying blast brain injuries, particularly mild and moderate, may be triggered by systemic, cerebrovascular and neuro-glia responses as consecutive but overlapping events.

INTRODUCTION

Medical, Social and Military Importance. The nature of warfare in the 21st century has led to a significant increase in primary blast or over-pressurization component of body injury which manifests as a complex of neuro-somatic damage, including traumatic brain injury (TBI), and often accompanied by posttraumatic stress syndrome (PTSD). Blast-related coalition fatalities, including IED, RPG, and rocket attacks, outnumber conventional fatalities during the last several years in Iraq and Afghanistan (**Fig. 1,** http://www.icasualties.org/). Moreover, for every blast-related fatality, many more soldiers suffer multiple, non-lethal blast exposures. This often leads to mild traumatic brain injury (mTBI), which is rarely recognized in a timely manner and has become a signature injury of the Iraq and Afghanistan conflicts (1-3).

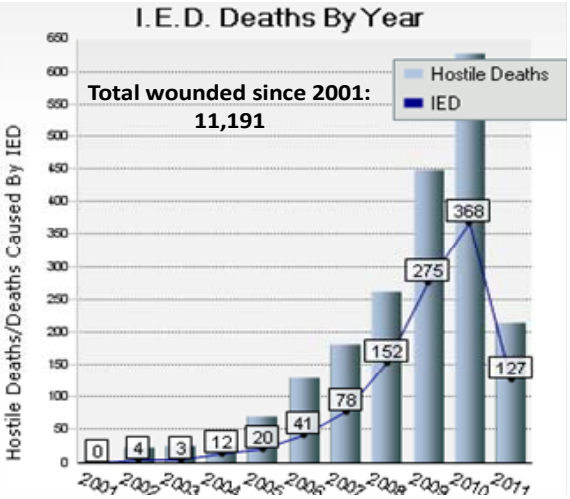

Fig. 1: Blast-related fatalities during OIF/OEF

Blast forces, particularly those that are repeated and low magnitude, are believed to produce minor but sustained disorders when neural damage cannot be detected or diagnosed by existing methods. Symptoms of mild or moderate blast brain injury often do not manifest themselves until sometime after the injury has occurred (4-6) and go undiagnosed and untreated because emergency medical attention is directed towards more visible injuries such as penetrating flesh wounds (7-9). However, even mild and moderate brain injuries can produce significant deficits and when repeated can lead to sustained neuro-somatic damage and neurodegeneration (4). Although exposure to repeated low level blasts is a common feature of war zones personnel/civilian population (OEF/OIF), the cumulative effect of multiple blasts on brain injury has not been investigated.

Data from our laboratories (10, 11) and others suggest that the mechanisms underlying such 'minor' injuries appear to be distinct from those imposed by mechanical impact or acceleration. Thus, identifying pathogenic mechanisms and biochemical markers of blast brain injury is vital to the development of diagnostics for mTBI through severe TBI. Validation of diagnostics and grading brain injury depending on the cumulative blast load will provide a dose-injury scale for personnel monitoring on the battlefield using portable blast "dosimeter" and/or a point of care diagnostic device.

Methodology and Results

Experimental Models for Studies of Blast Injury. Exposures to blast waves have the potential to inflict multi-system, including neurotrauma, as well as life threatening injuries to many personnel simultaneously (see (4) for review). It is generally accepted that primary blast injuries are generated as the over-pressurization wave propagates through the body causing damage at gas-fluid interfaces (12). The types of injuries inflicted include pulmonary barotraumas, tympanic membrane ruptures and middle ear damage, abdominal hemorrhage and perforation, rupture of the eye balls, and concussions (13).

A number of investigations have employed compressed air-driven shock tubes and nitrogen-driven blast wave generators for blast exposures of various animals (e.g. rats, mice, rabbits) to address mechanisms of injury (14-20). Small animals are placed in orthopedic stockinet slings, and large animals in open mesh Nylon TM slings, and subjected to blast exposure at varying distances and body orientations with or without a supportive/reflective plate behind the animal.

Our shock tube was designed and built to model a freely expanding blast wave as generated by a typical explosion **(see 11 for details)**. Blast injury modeling framework is shown in **Fig. 2.** Modular design allows for the flexibility to perform various types of tests: design is lightweight while maintaining necessary strength and stiffness. Data were acquired with PCB dynamic blast pressure transducers and LabView 8.2. Images were captured at 30 fps (frames per second) resolution. National Instruments 500,000 samples/sec data acquisition card were used to acquire data on multiple channels. Following the diaphragm rupture, the driver gas sets up a series of pressure waves in the low pressure driven section that coalesces to form the incident shockwave. In our shock tube, the burst pressure of the diaphragm separating the driver and driven sections do not change. Repeatability of diaphragm burst pressure was accomplished through the use of a cutter assembly directly in front of the diaphragm. Preliminary tests were conducted without animal specimens to optimize the peak overpressure (OP) and exposure time to accurately reproduce blast events: driver pressure and volume, diaphragm material, and shock tube exit geometry. Both static and dynamic (total) pressure was measured using piezoelectric blast pressure sensors/transducers positioned at the target. The shockwave recorded by blast pressure transducers in the driven section and at the target showed three distinct events: (i) peak overpressure, (ii) gas venting jet and (iii) negative pressure phase. Peak overpressure, positive phase duration, and impulse are the key parameters that correlate with injury and likelihood of fatality in animals and humans, for various orientations of the specimen relative to the blast wave (15, 16, 21-24). After the pressure history is recorded and the sensors removed, the animal can be carefully positioned at the same location and the test repeated, since it has been previously demonstrated that the proposed shock tube design has excellent repeatability characteristics.

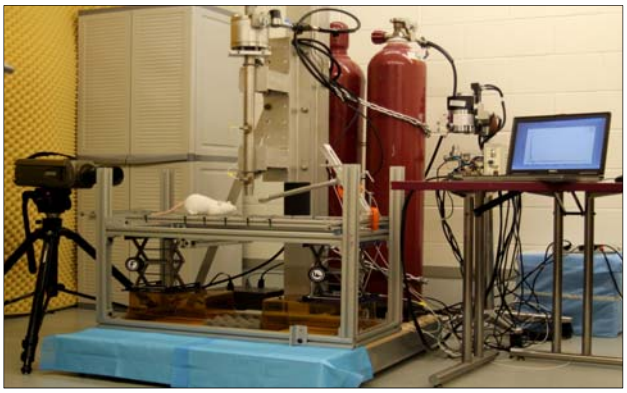

Fig.2 Overview of shock tube and experimental blast model facility at Banyan Biomarkers, Inc.

However, because of inconsistent designs among blast generators used in the different studies, the data on brain injury mechanisms and putative biomarkers have been difficult to analyze and compare. The main problem is that following blast peak overpressure, shock tubes immediately produce 'venting gas jet', substantially contaminating the blast wave **(Fig. 3).** Due to the complex nature of the blast event, the brain injury is a result of a combined impact of the "composite" blast including all 3 major phases of a shockwave shown in **Fig. 3 A and B**. Gas venting jet, albeit lower in magnitude than peak overpressure, lasts the longest, and represents the bulk of blast impulse and possibly produces the most devastating impact. We demonstrated previously a strong downward head acceleration following the passage of peak overpressure which lasts ~36 µsec (11). However, cranial deformation was more severe during the gas venting phase, lasting up to ~5-6 msec (Fig. 3A). These findings points to a potential flaw in several previous studies

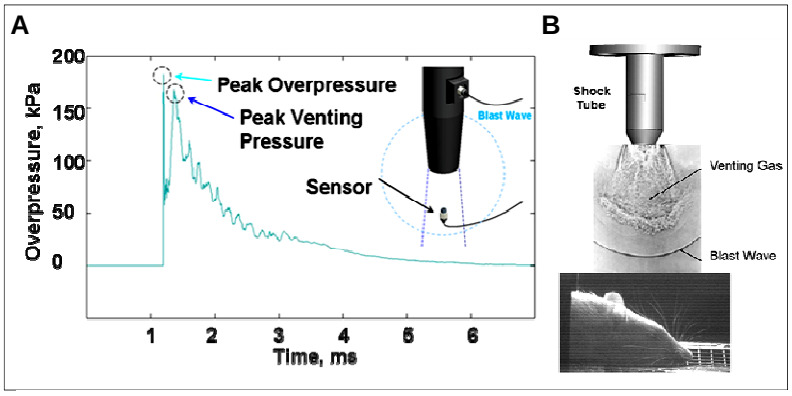

Fig. 3 Components of shock tube-generated shock wave. A: Peak overpressure and venting gas measured by PCB dynamic pressure sensors, and B: Rat head positioning relative to shock tube and visualization of shock wave using Schlieren optics

described in the literature: animal specimens are usually placed along the axis of the shock wave generator. In such location, the venting gas jet creates a much larger impulse (energy transfer) in the specimen than the peak overpressure itself. This effect can be virtually eliminated by placing rats off-axis from the venting jet in a way that the main effect acting on the specimen is the peak overpressure event.

Normal explosions produce blast winds that follow behind the incident shock. This effect is mimicked by shock tubes as the wave spherically expands. However, gas venting impulse is hard to control and it is probably not associated with the physics of primary blast event. A novel solution to address this problem is to place the target at an off-axis angle to avoid the venting altogether **(Fig. 4).**

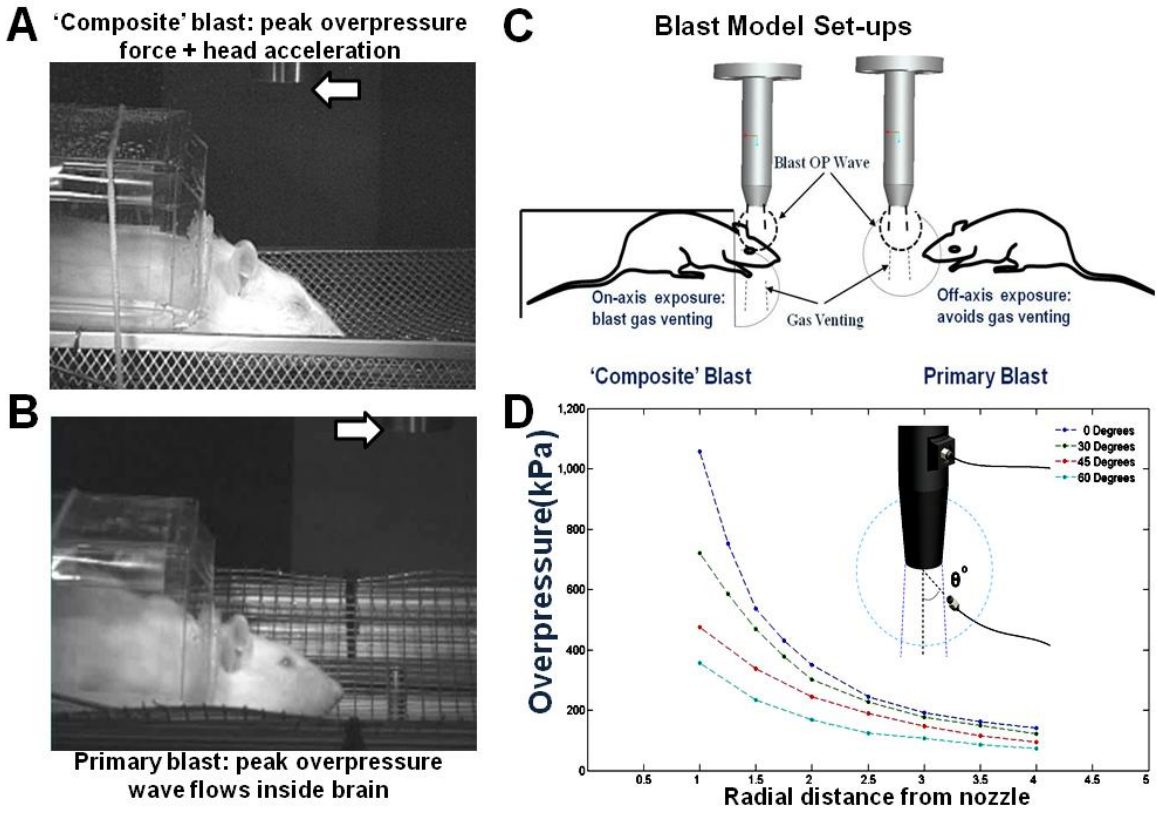

Fig. 4 Two general experimental set-ups for rat's exposure to shock tube-generated blast waves. A: on-axis of shock tube nozzle position: peak overpressure + venting gas produce head acceleration 'Composite blast'; B: off-axis position: blast wave peak overpressure only hitting rats; C graphic representation of two different set-ups; and D: Calibration of pressure on rat head depending on the angle and distance from the nozzle of shock tube.

The changing local speed of sound behind the wave causes the duration to increase with distance. For example, the 45° data shows duration increases from 53.1 to 85.3μs as the distance increases from 2D to 4D. By varying pressure settings, driven and driver lengths, and specimen location, independent control of blast overpressure, duration, and impulses may be achieved. Two different set-ups is shown in **Fig. 4.** We exposed rats to blast wave of a precisely controlled magnitude, duration and impulse at the surface of rat at various orientations of head to the blast wave with open or armored body: on axis and off-axis.

Molecular Components/Biomarkers of Blast-Induced Injury in Rats.

General hypothesis is that blast-induced brain injury is triggered and mediated by systemic, cerebrovascular, neuroinflammatory, neuroendocrine and neuro-glial responses as consecutive but overlapping events. Based on our previous global and targeted proteomic data, the following molecular components and injury biomarkers were assessed. Systemic/vascular responses: interleukin-1 and interleukin-10 (IL-1, IL-10), soluble intercellular adhesion molecule-1 (sICAM-1), L- and E-selectins. Glyosis was assessed by astrocytic marker GFAP and oligodendrocyte marker CNPase in both brain tissue and as biomarkers in serum. Neuronal injury was evaluated using brain tissue silver staining and serum levels of ubiquitin-C-terminal hydrolase UCH-L1 and Neuron-specific enolase (NSE). Neuroregenerative processes were evaluated by measuring brain tissue and serum levels of neuropilin-2 (NRP-2), receptor for VEGF and semaphorins.

Methods and Experimental Procedures. Neuroinjury and neurodegeneration was evaluated in the perfused and fixed brains using silver staining procedures at Neuroscience Associates (Knoxville, TN) utilizing the deOlmos Amino Cupric Silver Stain (http://www.neuroscienceassociates.com/Stains/silver_degen.htm). In addition, silver staining Kit from FD NeuroTechnologies was used where indicated (Ellicott City, MD). GFAP and CNPase immunohistochemistry was performed using mouse mAbs (Cell Singaling) and visualized using DAB Vector Labs Kit. Serum content of IL-1, IL-10, Integrin α/β, L- and E-selectins, Fractalkine, and Neuropilin-2 were measured using rat Quantibody array (Ray Biotech, GA USA). Also, sICAM and L-selectin were quantified independently using SW ELISA Kits. In addition, Neuropilin-2 and CNPase levels in serum and expression in brain was analyzed by Western blot with corresponding antibodies (Cell Signaling, Abcam) and bands were calculated using ImageJ software. Amounts of GFAP and UCH-L1 in serum were determined using SW ELISA Kits developed at Banyan Biomarkers, Inc., and NSE was assayed by rat-specific SW ELISA (Life Sciences Advanced Technologies, Saint Petersburg, FL).

Silver staining of neurodegeneration level in rat brain after different blast exposures. Rats were subjected to (i) 'composite' head-directed severe blast exposure (52 psi/10 msec total) on axis (body protected) accompanied by strong head movement; (ii) off-axis (30' degree) exposure to the blast of same shock tube settings resulted in 33.9 psi peak overpressure at the middle of frontal head **(Fig. 4 C)** lasted for 113 microseconds; and (iii) controlled cortical impact (CCI) of 2.0 mm depth.

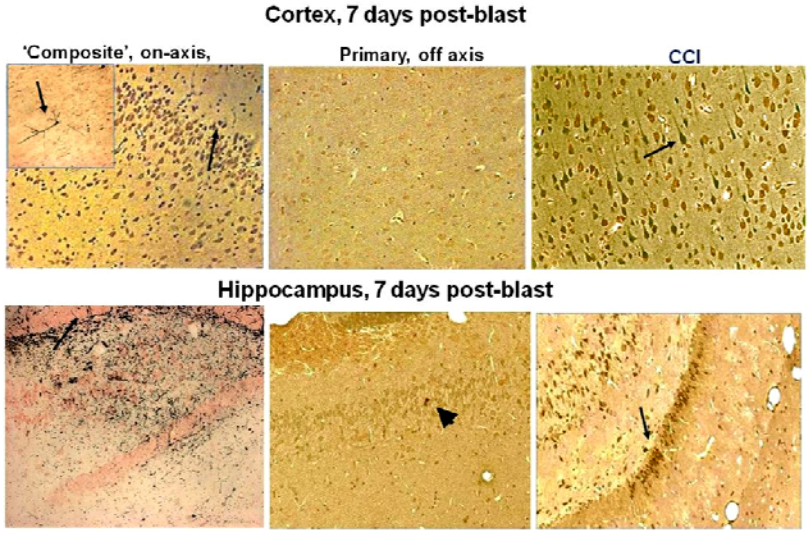

Fig. 5 Silver staining in coronal sections of midbrain (mesencephalon). Positive silver accumulation accumulation is indicated by arrows. Inset (cortex composite) shows degenerated neuron. Arrowhead in hippocampus after primary blast points on possible silver accumulation in the cell.

As can be seen in **Fig. 5,** on-axis blast produces significant silver accumulation at 7 day post-blast, particularly in hippocampus (indicated by arrows). CCI also results in positive staining in ipsilateral cortex and hippocampus. In contrast, there was a rare occurrence of silver accumulation observed in cortex or hippocampus after exposure to primary blast (arrowhead).

Serum levels of NSE and UCH-L1 as biomarkers of neuronal injury after different blast exposures. Rats were exposed to on-axis single composite blast of 52 psi, 10 msec total duration of positive phase + venting gas. Serum NSE **(Fig. 6A)** and UCH-L1 **(Fig. 6B)** were measured using SW ELISA Kits.

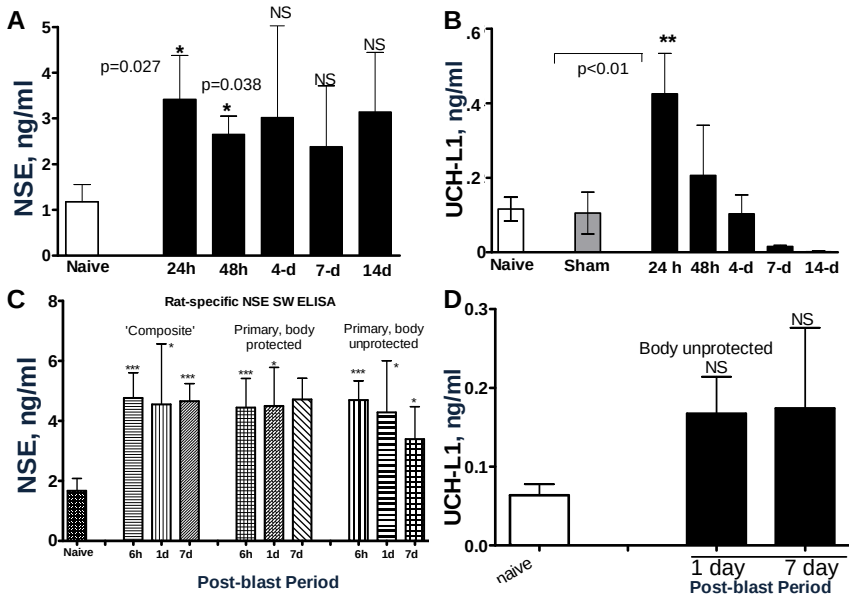

Fig. 6 NSE and UCH-L1 accumulation in blood after different types of blast exposure. A, B: serum NSE and UCH-L1 after on-axis 'Composite blast'; C, D: serum NSE and UCH-L1 after off-axis primary blast; Mean + SEM are shown of at least 3 rats per point from each group performed in duplicate. Unpaired t-test was employed to analyze statistical significance of values. *p<0.05, ** p<0.01; ***, p<0.005

The same settings of shock tube were used to challenge rats to off-axis primary blast (30^{o} degree from nozzle) with PO 33.9 psi, duration of 113 µsec registered at the head with body covered or unprotected as indicated.

NSE was significantly elevated in serum within first 24-48 hours after composite blast **(Fig. 6A)**, and the increase trend persisted up to 14 day although was not statistically significant (n=4 rats in each group). In this set of experiments, NSE SW ELISA Kit (Alpha Diagnostics), which was not specifically designed for rat NSE, was employed. In the subsequent sets of experiments **(Fig. 6C)**, we used NSE SW ELISA Kit from Life Sciences Advanced Technologies designed to detect specifically rat NSE. As can be seen in **Fig. 6A**, remarkable accumulation of NSE was detected in serum within 6 hours following exposure to either 'composite' or primary blast. NSE increase sustained up-to 14 days post-blast interval. Serum UCH-L1 elevated at 24 hours after 'composite' blast followed by a rapid decline **(Fig. 6B)**. Increases in serum UCH-L1 were not statistically significant after a single primary blast exposure (n=4), although an elevation trend could be detected **(Fig. 6B)**. Studies of NSE and UCH-L1 as serum biomarkers after multiple blast exposures of various magnitude are under way.

Serum levels of GFAP as marker of glyosis (astrocytes). GFAP was increased within 24 hours after composite blast and rapidly returned to baseline at 4-14 days **(Fig. 7A)**. While there was a significant increase of GFAP after primary blast at body protected and open (partially), the magnitude of increase was lower than after composite blast. In contrast, the GFAP increases lasted for 7 days following primary but not composite blast exposures **(Fig. 7 A, B)**.

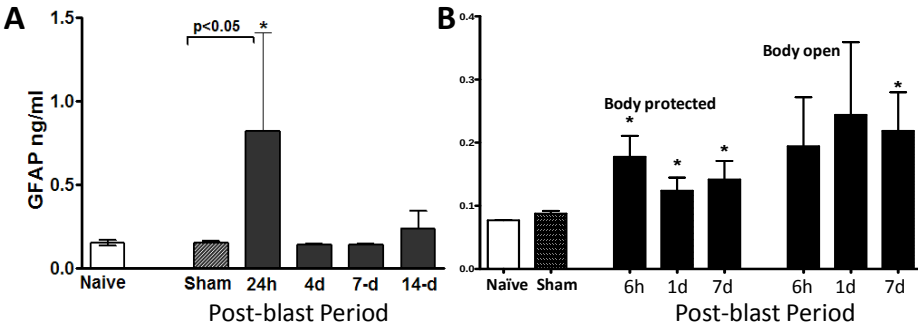

Fig. 7. GFAP levels in blood after different blast exposures. A: serum GFAP after on-axis 'Composite blast'; B: serum GFAP after off-axis primary blast; On axis: Unpaired t-test was employed to analyze statistical significance of values. (*-p<0.05; **-p<0.01). Off axis: t-test with Welch correction was done. (*-p<0.05), Mean + SEM of values from 3 to 5 rats per point is shown.

Cytokine/Chemokine responses after blast exposures. We hypothesized that systemic and neuroinflammmation together with impaired vascular reaction in the brain, result in enhancement of endothelial permeability/leakage, infiltration of macrophages from circulation and activation of brain-resident microglia cells:

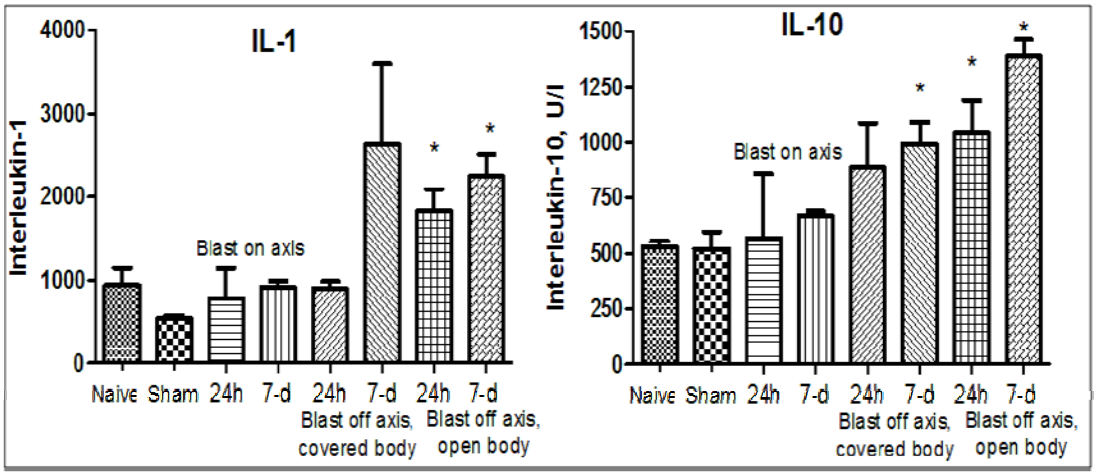

Fig. 8. Serum IL-1 and IL-10 at different times post-blast on- and off-axis. Note: the most prominent response occurs when OP wave 'flows inside the brain'- off axis frontal exposure with open body. *=p<0.05 vs. naïve/sham was considered as statistically significant according to unpaired t-test, NS-Not significant

As can be seen in **Fig. 8,** both pro-inflammatory (IL-1) and counteracting anti-inflammatory molecules (IL-10) accumulate in circulation at 24 hour after open body exposure to frontal (off-axis) blast.

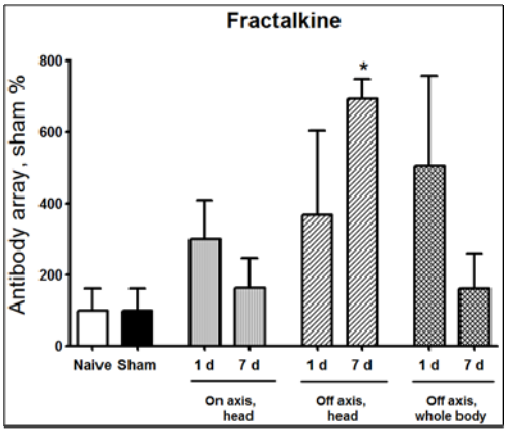

These results are in agreement with data obtained using non-blast TBI models (25). Moreover, CX3CL1 chemokine Fractalkine was also significantly elevated after different types of blast further suggesting systemic component in response to blast **(Fig. 9)** consistent with reports on the level of this chemokine in patients with TBI and in mouse model of closed head injury (26).

Fig. 9 . Levels of Fractalkine after different types of blast. *p<0.05, t-test, NS-not significant

Vascular responses and dysregulation of cell adhesion molecules. E-selectin and L-selectin as bridges connecting vascular-endothelial-neural tissue disturbances.

E-selectin and L-selectin are adhesion molecules which characterize the activation of vascular component of inflammation and interaction of circulatory cells with endothelial component of blood-brain-barrier (BBB) (27).

As can be seen in **Fig. 10**, the most prominent activation of vascular components of blast responses occurs when peak overpressure interacts with the frontal part of head without significant acceleration: "flowing blast insight the brain" (blast off-axis open body).

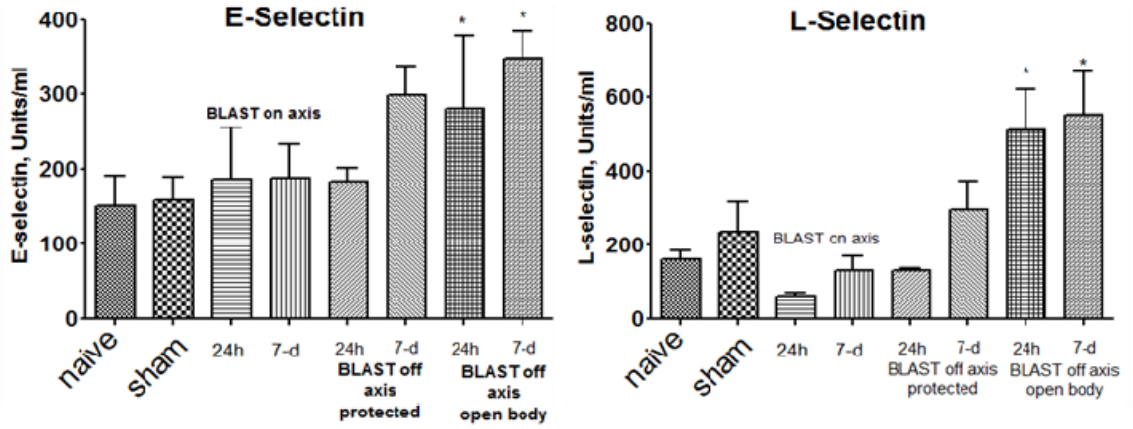

Fig. 10 Levels of L-selectin and E-selectin in serum after different types of blast exposure. Rats were subjected to off-axis head + total body blast: 33.9psi, 113 msec, 10.6 kPa-sec with body armored or uncovered. Blood was collected and cytokines were assayed in serum using RayBiotech L-arrays and expressed in arbitrary Units/ml. Data are Mean+SEM of 3 independent experiments (rats), each assay performed in triplicate. *=p<0.05 vs. sham (noise exposed rats) according unpaired t-test analysis. NS- Not significant.

Using targeted approach, we identified additional component of neurotrophic response to blast exposure. Serum levels of Nerve Growth Factor beta (beta-NGF) was assessed using SW ELISA and Neuropilin-2 (NRP-2) by antibody array (Ray Biotech) after blast exposure at different set-up. The results are presented in **Fig. 11A and B** below.

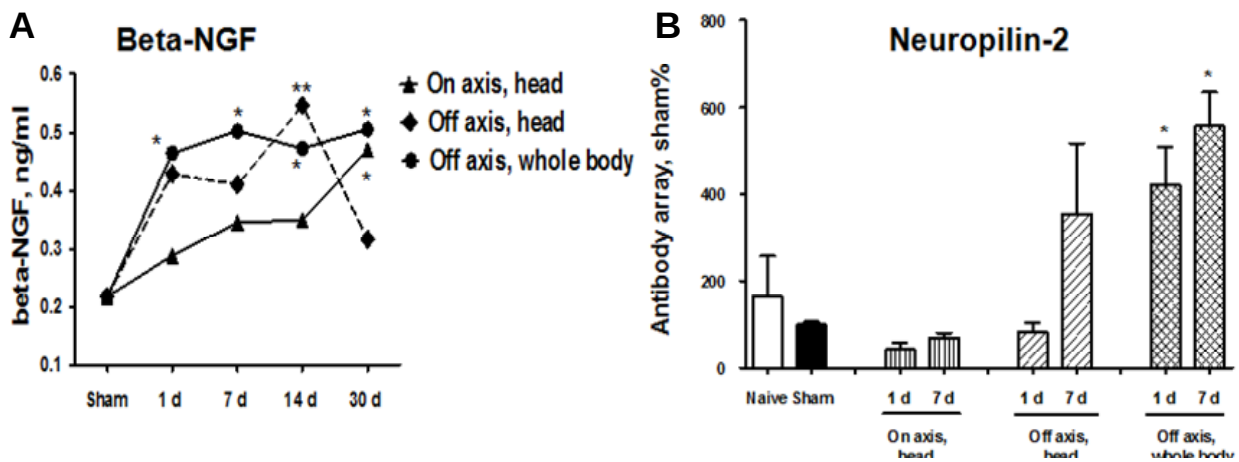

Fig. 11. Time-course of serum beta-NGF (A) and NRP-2 (B) following on-axis vs. off axis positions (primary blast overpressure only). Data point represents Mean values of 3 rat samples from each group and time points. *-p<0.05 and **-p<0.01 vs. sham group according to unpaired t-test with Welch correction.

Beta-NGF has been suggested to play a neurotrophic role in several neurodegenerative diseases (*39-41*). Our data indicate that NGF may also have neuroprotective functions and be involved in adaptive responses/neurorepair after blast induced TBI. As can be seen, exposure of whole body to primary overpressure blast instigated a rapid and sustained accumulation of beta-NGF in serum. Neuropilin-2 is receptor for VEGF and semaphorins, a large family of secreted and transmembrane signaling proteins that

regulate axonal guidance in the developing CNS (*42-44*). Our preliminary data **(Fig. 11B**) suggest that predominantly primary blast activates neuroregeneration and that NRP-2 may be involved in this process. Studies are under way to determine diagnostic and/or prognostic roles for NRP-2 in multiple low level blast as well as mechanisms of blast stimulation of neural injury/repair.

In summary, the most profound and persistent changes in serum levels of NSE/UCH-L1, GFAP were observed upon composite blast. However, prominent systemic and persistent glial up-regulation was observed after primary blast particularly when the total animal body was subjected to blast exposures. We suggest that the mechanisms underlying blast brain injuries, particularly mild and moderate, may be triggered by systemic, cerebrovascular and neuro-glia responses as consecutive but overlapping events. More in detail investigation is required to delineate primary blast injury from peak overpressure and distinguish from 'composite' blast. The pathophysiological signatures of mild/moderate blast, particularly cumulative effects of multiple exposures remain to be elucidated.

References.

1. Jones, E., Fear, N.T., and Wessely, S. 2007. Shell shock and mild traumatic brain injury: a historical review. *Am J Psychiatry* 164:1641-1645.
2. Terrio, H., Brenner, L.A., Ivins, B.J., Cho, J.M., Helmick, K., Schwab, K., Scally, K., Bretthauer, R., and Warden, D. 2009. Traumatic brain injury screening: preliminary findings in a US Army Brigade Combat Team. *J Head Trauma Rehabil* 24:14-23.
3. Warden, D. 2006. Military TBI during the Iraq and Afghanistan wars. *J Head Trauma Rehabil* 21:398-402.
4. Cernak, I., and Noble-Haeusslein, L.J. 2009. Traumatic brain injury: an overview of pathobiology with emphasis on military populations. *J Cereb Blood Flow Metab*.
5. Cernak, I., Savic, J., Ignjatovic, D., and Jevtic, M. 1999. Blast injury from explosive munitions. *J Trauma* 47:96-103; discussion 103-104.
6. Yilmaz, S., and Pekdemir, M. 2007. An unusual primary blast injury Traumatic brain injury due to primary blast injury. *Am J Emerg Med* 25:97-98.
7. Belanger, H.G., Scott, S.G., Scholten, J., Curtiss, G., and Vanderploeg, R.D. 2005. Utility of mechanism-of-injury-based assessment and treatment: Blast Injury Program case illustration. *J Rehabil Res Dev* 42:403-412.
8. Nelson, T.J., Wall, D.B., Stedje-Larsen, E.T., Clark, R.T., Chambers, L.W., and Bohman, H.R. 2006. Predictors of mortality in close proximity blast injuries during Operation Iraqi Freedom. *J Am Coll Surg* 202:418-422.
9. Wolf, S.J., Bebarta, V.S., Bonnett, C.J., Pons, P.T., and Cantrill, S.V. 2009. Blast injuries. *Lancet* 374:405-415.
10. Svetlov, S.I., Larner, S.F., Kirk, D.R., Atkinson, J., Hayes, R.L., and Wang, K.K. 2009. Biomarkers of blast-induced neurotrauma: profiling molecular and cellular mechanisms of blast brain injury. *J Neurotrauma* 26:913-921.
11. Svetlov, S.I., Prima, V., Kirk, D.R., Gutierrez, H., Curley, K.C., Hayes, R.L., and Wang, K.K.W. 2009. Morphologic and biochemical characterization of brain injury in a model of controlled blast overpressure exposure. *Journal of Trauma* 2010, 69(4) 795-804.

12. Born, C.T. 2005. Blast trauma: the fourth weapon of mass destruction. *Scand J Surg* 94:279-285.

13. Wightman, J.M., and Gladish, S.L. 2001. Explosions and blast injuries. *Ann Emerg Med* 37:664-678.

14. Guy, R.J., Glover, M.A., and Cripps, N.P. 1998. The pathophysiology of primary blast injury and its implications for treatment. Part I: The thorax. *J R Nav Med Serv* 84:79-86.

15. Jaffin, J.H., McKinney, L., Kinney, R.C., Cunningham, J.A., Moritz, D.M., Kraimer, J.M., Graeber, G.M., Moe, J.B., Salander, J.M., and Harmon, J.W. 1987. A laboratory model for studying blast overpressure injury. *J Trauma* 27:349-356.

16. Stuhmiller, J.H. 1997. Biological response to blast overpressure: a summary of modeling. *Toxicology* 121:91-103.

17. Stuhmiller, J.H., Ho, K.H., Vander Vorst, M.J., Dodd, K.T., Fitzpatrick, T., and Mayorga, M. 1996. A model of blast overpressure injury to the lung. *J Biomech* 29:227-234.

18. Cernak, I., Wang, Z., Jiang, J., Bian, X., and Savic, J. 2001. Cognitive deficits following blast injury-induced neurotrauma: possible involvement of nitric oxide. *Brain Inj* 15:593-612.

19. Chavko, M., Koller, W.A., Prusaczyk, W.K., and McCarron, R.M. 2007. Measurement of blast wave by a miniature fiber optic pressure transducer in the rat brain. *J Neurosci Methods* 159:277-281.

20. Chavko, M., Prusaczyk, W.K., and McCarron, R.M. 2006. Lung injury and recovery after exposure to blast overpressure. *J Trauma* 61:933-942.

21. Cooper, G.J., and Taylor, D.E. 1989. Biophysics of impact injury to the chest and abdomen. *J R Army Med Corps* 135:58-67.

22. Cooper, P.W. 1996. *Explosives Engineering*: Wiley-VCH.

23. Elsayed, N.M. 1997. Toxicology of blast overpressure. *Toxicology* 121:1-15.

24. Elsayed, N.M., and Gorbunov, N.V. 2007. Pulmonary biochemical and histological alterations after repeated low-level blast overpressure exposures. *Toxicol Sci* 95:289-296.

25. W. D. Dietrich, K. Chatzipanteli, E. Vitarbo, K. Wada, K. Kinoshita, The role of inflammatory processes in the pathophysiology and treatment of brain and spinal cord trauma. Acta Neurochir Suppl 89, 69 (2004).

26. H. Ralay Ranaivo, S. Zunich, N. Choi, J. Hodge, M. Wainwright, Mild stretch-induced injury increases susceptibility to interleukin-1β-induced release of matrix metalloproteinase-9 from astrocytes. J Neurotrauma, 2011 (Jul 6) Epub ahead of print .

27. M. J. Whalen et al., Reduced brain edema after traumatic brain injury in mice deficient in P-selectin and intercellular adhesion molecule-1 J Leukoc Biol 67, 160 (Feb, 2000).

28. P. Calissano, C. Matrone, G. Amadoro, Nerve growth factor as a paradigm of neurotrophins related to Alzheimer's disease. Dev Neurobiol 70, 372 (Apr, 2010).

29. P. Bannerman et al., Peripheral nerve regeneration is delayed in neuropilin 2-deficient mice. J Neurosci Res 86, 3163 (Nov 1, 2008).

30. J. Roffers-Agarwal, L. S. Gammill, Neuropilin receptors guide distinct phases of sensory and motor neuronal segmentation. Development 136, 1879 (Jun, 2009).

Experimental Framework for Cumulative Blast Detection and Data Acquisition for Assessment of Blast-Related Injury in Animal Studies

Year 2, Progress Report No. 3 (Revised)

Hector Gutierrez and Daniel Kirk

Department of Mechanical and Aerospace Engineering

Florida Institute of Technology

Melbourne FL 32901

April 16, 2012 / October 21, 2012

Experimental Framework for Cumulative Blast Detection and Data Acquisition for Assessment of Blast-Related Injury in Animal Studies

Year 2 – Report 3 (Revised).

Introduction.

The experiences gained during Year 1 of this project pointed in the direction of two critical aspects of the instrumentation, data acquisition and data logging technology. First, a sensing device with response time below 1 microsecond must be used to properly capture the peak overpressure, since it's believed that one of the mechanisms of injury is related to the exact value of peak overpressure. Second, the data acquisition and data logging electronics have to be fast enough to properly capture a sub-microsecond event, which is very challenging considering that the size of the devices is ideally in the order of one inch square (to be usable in rodent testing).

To capture a blast event where the peak overpressure lasts only 1~3 microseconds, a sensor with frequency response in excess of 1 MHz is needed. Candidate technologies must be compact enough such that both the sensing element and the conditioning electronics can fit on a printed circuit board of approx. 1 inch square in area. A candidate sensor element based on a piezo disc has been used to develop a dedicated sensor for the CBI-ESP sensor package.

This report describes the development and testing of a new piezo-based portable high-speed blast sensor, and presents its results in monitoring blast exposure on a rodent.

Piezo electric sensors

Piezoelectric transducers can be used in conjunction with board-level signal conditioning to develop a very compact micro transducer with frequency response comparable to that of the fastest pressure transducers currently available. Piezo materials generate an electrical charge that is proportional to the pressure applied. If a reciprocating force is applied, an ac voltage is seen across the terminals of the device. Piezoelectric sensors are not suited for static or dc applications because the electrical charge produced decays with time due to the internal impedance of the sensor and the input impedance of the signal conditioning circuits. However, they are well suited for dynamic or ac applications.

Signal Conditioning for piezo-electric sensors

Key items to consider when designing a piezo signal conditioner are:

- Frequency of operation
- Signal amplitude
- Input impedance
- Mode of operation

The high impedance of the sensor requires an amplifier with high-input impedance. JFET or CMOS input op amps, like the TLV2771, are natural choices. Two circuit approaches were tested for signal conditioning. Figure 1 shows a voltage mode amplifier circuit, which was selected as the best choice. Voltage mode amplification is used when the amplifier is very close to the sensor, charge mode amplification is used when the amplifier is remote to the sensor.

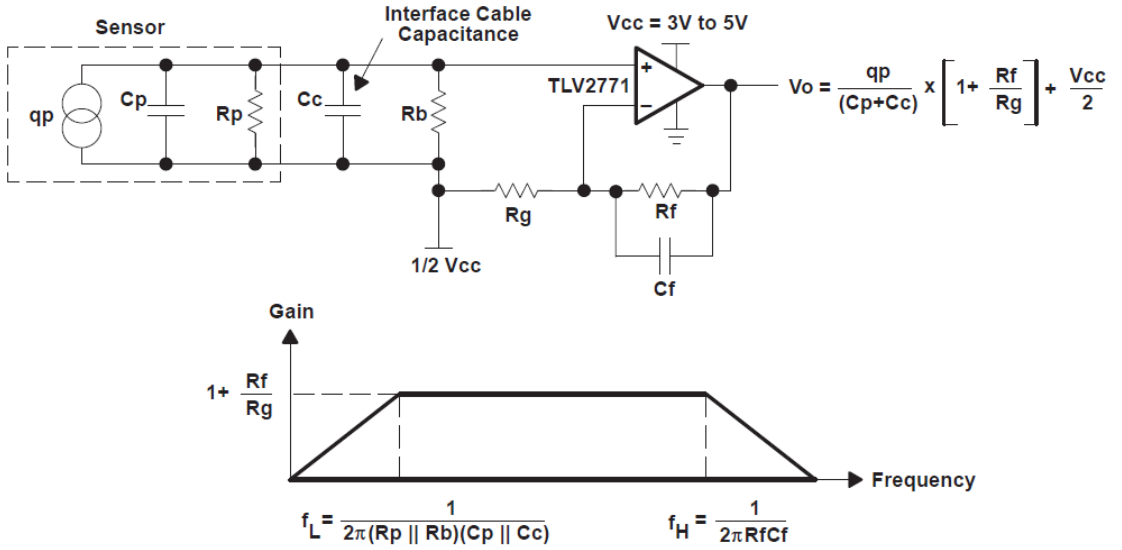

Figure 1. Voltage mode signal conditioner for a piezoelectric sensing element

In a voltage mode amplifier, the output depends on the amount of capacitance seen by the sensor. In the charge mode amplifier the charge injected into the negative input is balanced by charging the feedback capacitor Cf.

Usually it is difficult to get enough sensitivity and bandwidth using a single gain stage. Therefore it is usually necessary to amplify signal in two successive stages. If both the first and second stages are inverting amplifiers, so polarity (phase) of the signal is corrected. A high pass filter before the input of second stage Op-Amp is placed to eliminate the DC offset generated by the first stage Op-Amp. A low pass filter is placed to attenuate the peak sensitivity at the resonant frequency. In an application that requires a wide flat sensitivity band, it may be difficult to get enough attenuation by a low order low pass filter and cascaded filters can be used, at the expense of additional phase delay.

The work in the last quaternary period has been focused on prototyping, debugging and bench testing several circuit topologies to find one that meets all the requirements of the CBI-ESP application. The approaches previously discussed have been combined to implement a conditioning circuit that has the required performance for the CBI-ESP high-speed portable sensor package. During the prototype stage the signal conditioning circuits were tested using bench top signal generators, prior to final testing with blast events. The proposed signal conditioner circuits have been tested with three types of waveforms:

- Sinusoidal waveforms at 1 kHz, 10 kHz, 100 kHz, 1 MHz
- Triangular waveforms at 1 kHz, 10 kHz, 100 kHz, 1 MHz
- Pulse waveforms at 10 kHz, 100 kHz, 400 kHz

Results from these tests are shown in Figures 2, 3, 4, 5, 6 and 7. The current prototype performs very well with a flat gain response (x16) up to 400 kHz; the gain rolls of to x12 at 1 MHz. It is estimated that to properly capture (with no scale distortion) the peak overpressure of a blast event, the circuit needs a flat gain response in excess of 1.2 MHz, which has been achieved with the current prototype.

Another development task during the last period of performance has been to identify and procure sensor candidates for the CBI-ESP device. The sensor candidates have to meet the size and frequency response requirements of the CBI-ESP: they have to be flat, able to be surface mounted on a 1 inch x 1 inch printed circuit board, and have frequency response in excess of 1 Mhz. The following sensors that meet all these requirements have been identified and purchased:

- Piezoelectric disks, from Steiner and Martins, Inc.
  Four different piezoelectric sensing elements have been procured: 1.7 MHz (15 x 1.2 mm), 3.4 MHz (12 x 0.6 mm), 3.5 MHz (9 x 0.5 mm) and 5 MHz (10 x 0.4 mm).

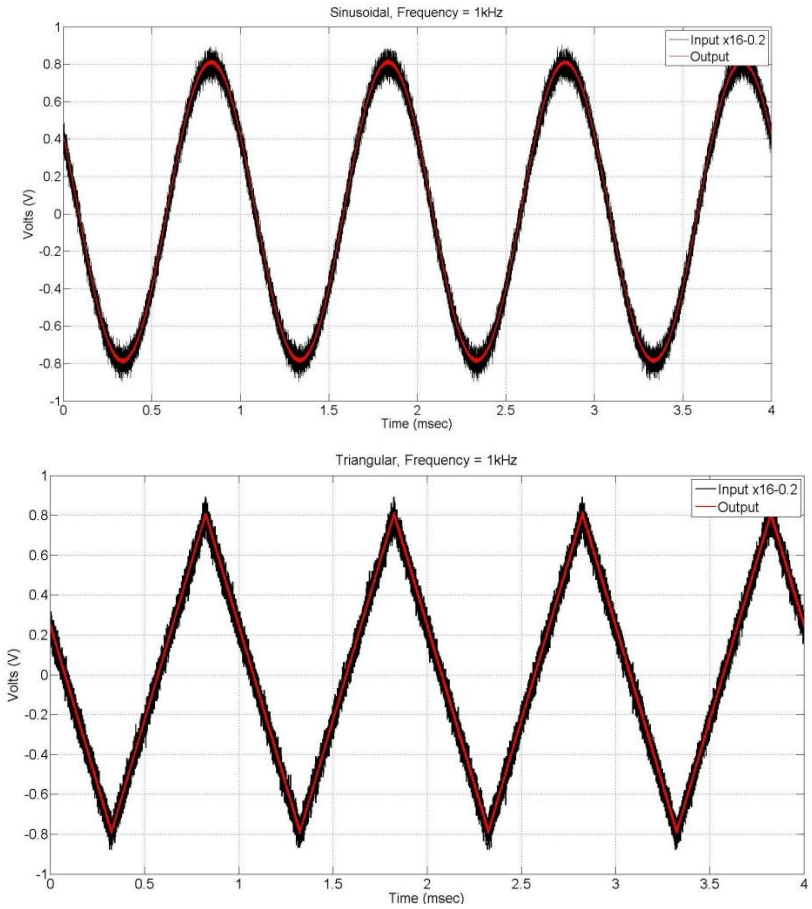

Figure 2. Response of the CBI-ESP signal conditioner circuit prototype to sine waves and triangular waveforms at 1 kHz.

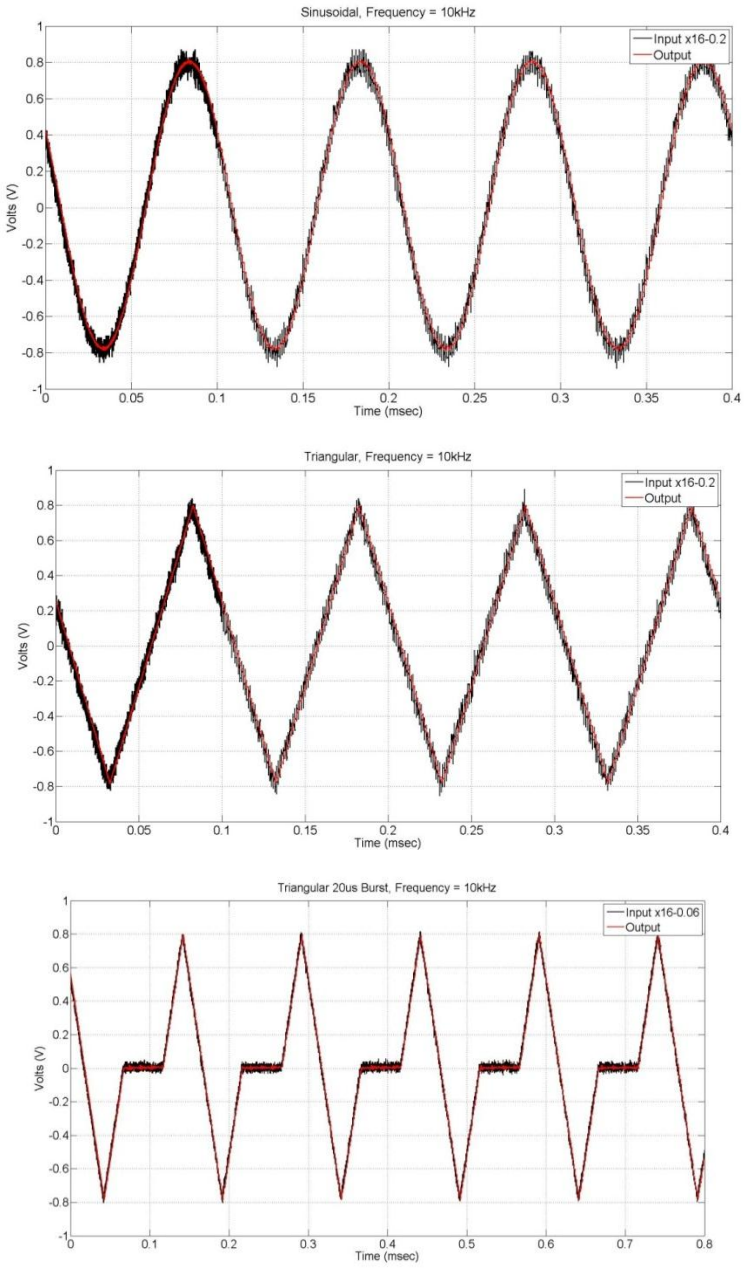

Figure 3. Response of the CBI-ESP signal conditioner circuit prototype to sine waves, triangular waveforms and pulse waveforms at 10 kHz.

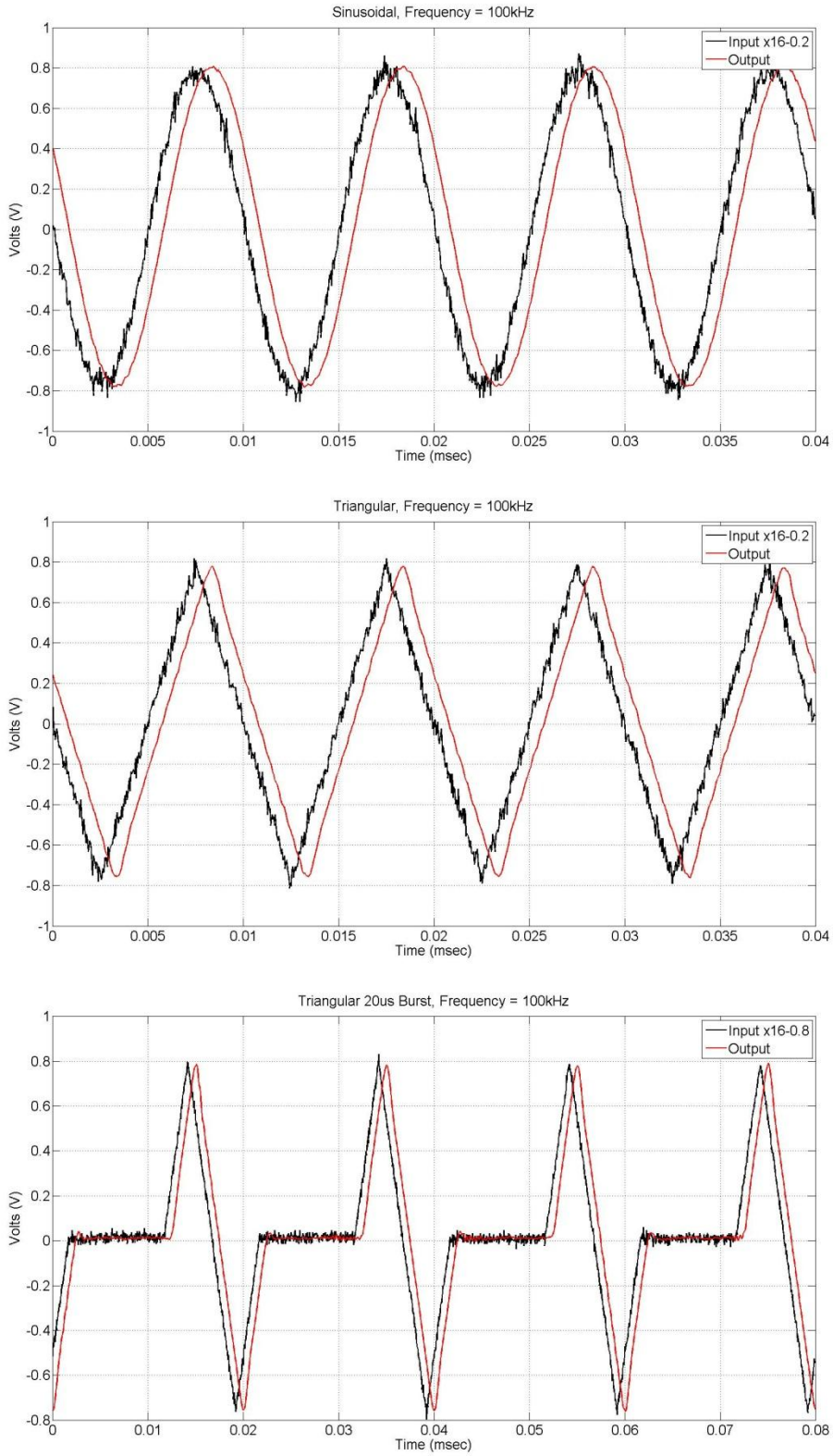

Figure 4. Response of the CBI-ESP signal conditioner circuit prototype to sine waves, triangular waveforms and pulse waveforms at 100 kHz.

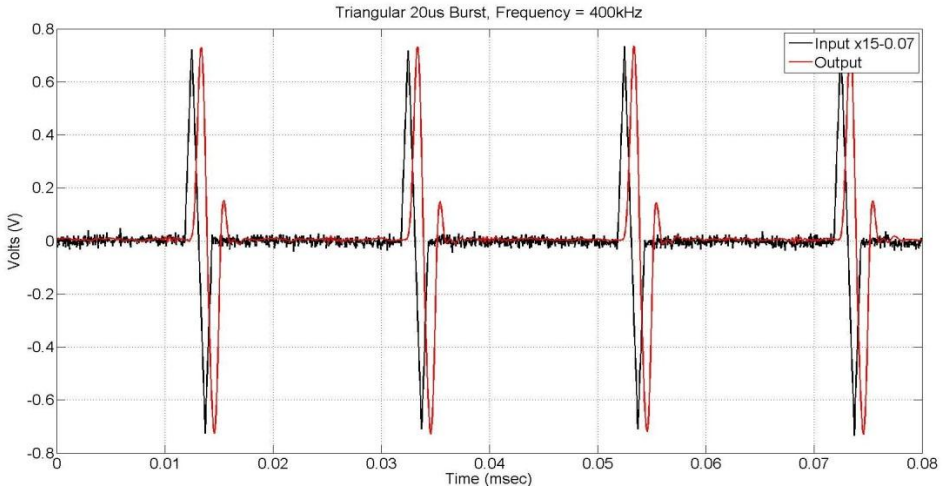

Figure 5. Response of the CBI-ESP signal conditioner circuit prototype to pulse waveforms at 400 kHz.

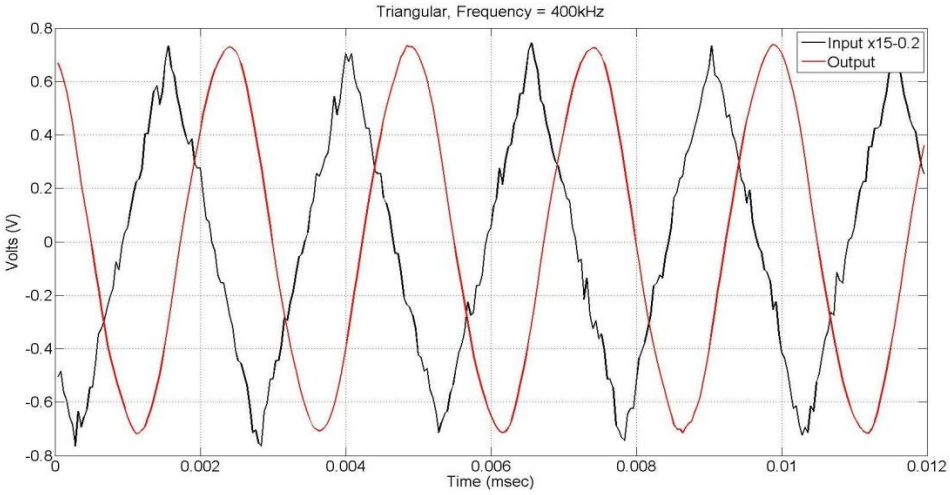

Figure 6. Response of the CBI-ESP signal conditioner prototype to triangular waveforms at 400 kHz.

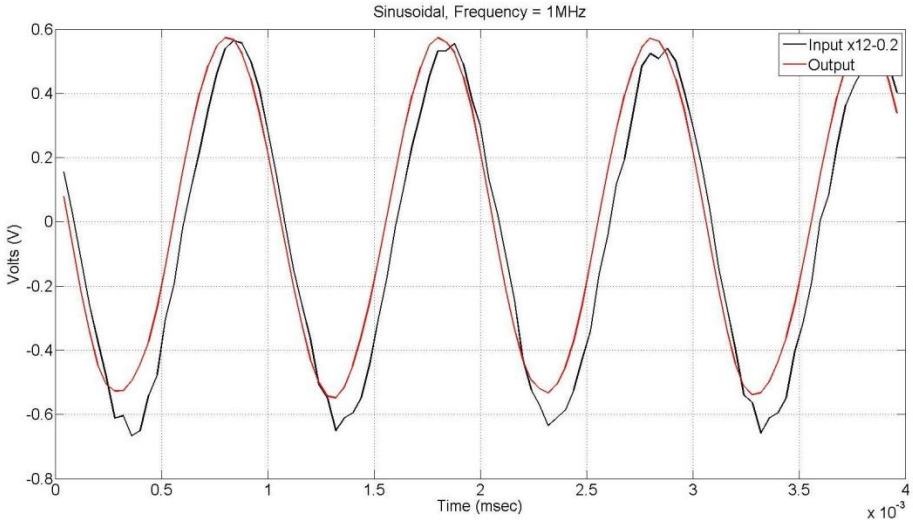

Figure 7. Response of the CBI-ESP signal conditioner prototype to sinusoidal waveforms at 1 MHz.

Tests at Banyan Biomarkers

The prototype sensor and signal conditioning circuit were tested at Banyan Biomarkers on 19 October 2012. The sensor and conditioning circuits were tested as follows:

- Both the FIT prototype and PCB benchmark sensor in parallel configuration (Figure 8). Eight tests were conducted at different radial distances from the opening of the shock tube to characterize sensitivity of the FIT prototype at different peak pressures (Figure 12).
- FIT prototype on toy rat in triangular configuration to verify approximate peak pressure level on test specimen prior to the live test (Figure 9)
- FIT prototype and PCB benchmark sensor in triangular configuration, to deliver repeated blast exposure to laboratory animal (three tests, 30 min apart). (Figure 10).

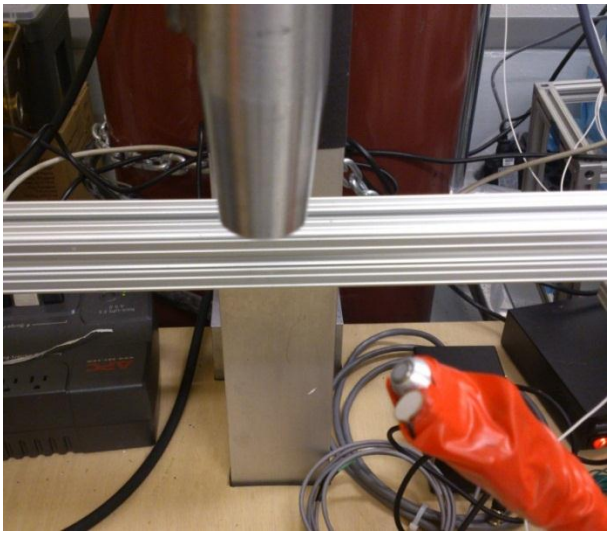

Figure 8. Parallel configuration, PCB sensor (up) and FIT prototype (down)

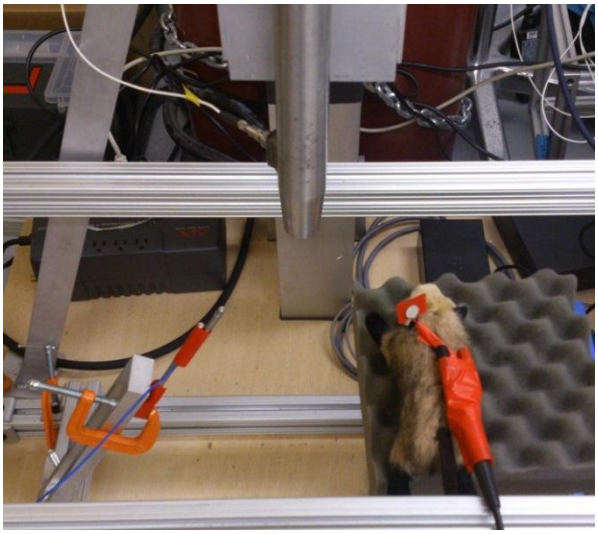

Figure 9. Triangular configuration to verify peak overpressure on target location prior to animal tests

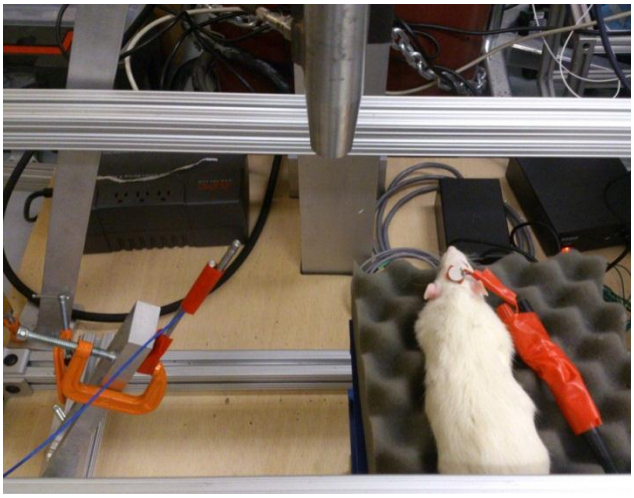

Figure 10. Triangular configuration for animal testing including both PCB benchmark sensor (left) and FIT sensor prototype (right, on animal's head)

Results

The prototype sensor and signal conditioning circuit demonstrated fast enough response to accurately detect the peak overpressure as compared to the benchmark PCB sensor. The results are shown in Figure 11, 12 and 13. All tests were conducted at a sampling rate of 10 Msamples/sec/channel using a PXI data acquisition chassis from National Instruments.

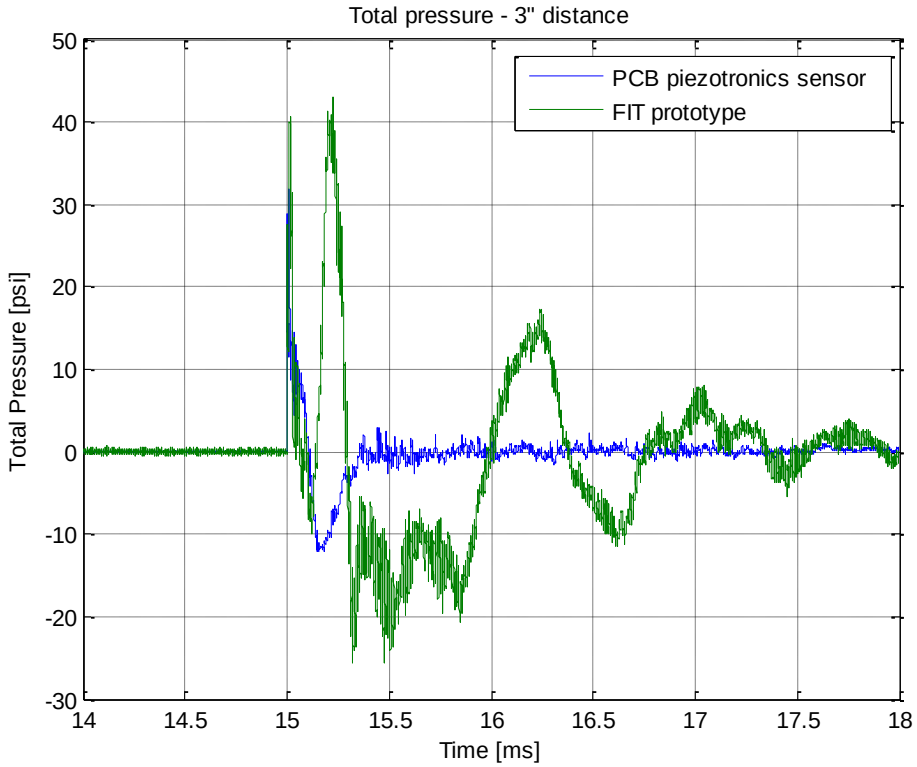

Figure 11. Typical pressure trace of the FIT prototype compared to the PCB benchmark sensor

Figure 11 shows a typical pressure trace obtained with the FIT prototype sensor and signal conditioner (green trace) compared to the PCB benchmark sensor (blue trace). The plot shows that both sensors can capture the peak overpressure event at the same time and with the same intensity (as converted from volts to psi).

Both the PCB pressure sensor and the FIT prototype suffer from resonant ringing at a frequency that depends on both the material and construction of the sensor. This is typical of all piezoelectric-based sensing systems, and can be compensated by off-line data post processing assuming that the signal was sampled at high enough frequency to avoid aliasing. In our case, the piezo resonances are at 200 kHZ (for the FIT prototype) and 250 kHz (for the PCB sensor), which considering our sampling rate of 10 Msamples/sec/channel provide ample margin for accurate off-line digital filtering.

The ringing frequency was measured in both the PCB and FIT sensors and found to be constant for all testing conditions, as shown in Figure 12. This confirms that the ringing frequency is characteristic of the sensor material and geometry and is not affected by the test conditions.

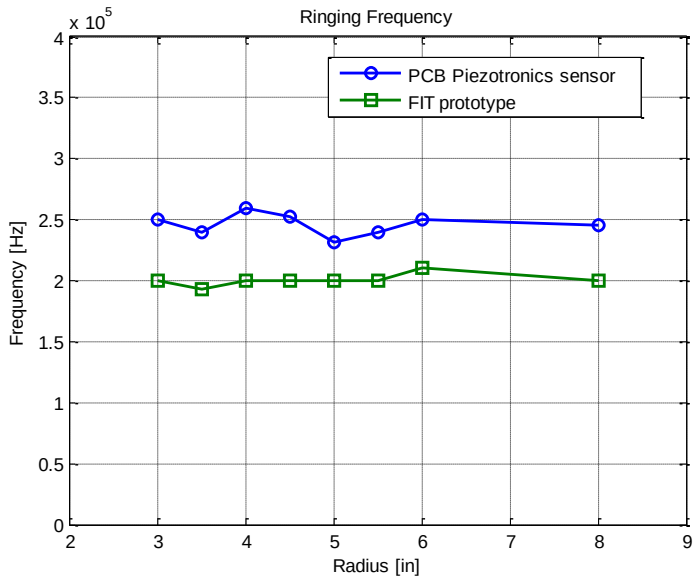

Figure 12. Measured resonant frequency of both sensor systems for different distances to the shock tube opening

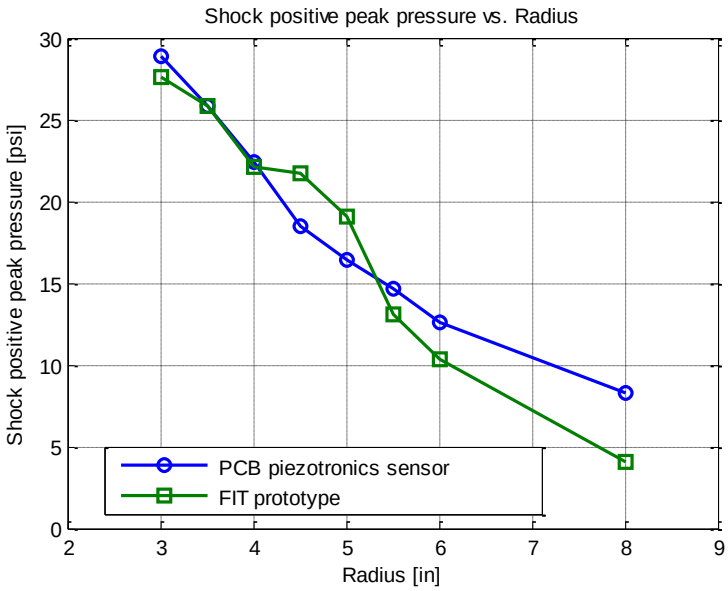

Figure 13. Positive peak pressure (psi) of both sensor systems for different distances to the shock tube opening

Figure 13 shows the correlation between positive peak pressure and distances to the shock tube opening for both the PCB and FIT sensor systems. This shows that the FIT system is capable of measuring the peak overpressure of the blast event. These test will be repeated on an improved test rig to further demonstrate the performance of the FIT sensor system under more geometrically accurate placing.

Conclusion.

The FIT prototype sensor and signal conditioning circuit have been designed, built and successfully tested. The proposed prototype has demonstrated enough response speed to accurately record the peak overpressure of the blast event as compared to the benchmark PCB sensor. Further tests on an improved test rig will help to further demonstrate the performance of the FIT sensor using a better method to accurately place both sensors in the field of the blast relative to each other and to the blast axis.

Ringing has been detected on both the PCB and FIT sensors, as expected on any piezo electric devices operating under blast conditions. The ringing frequency is constant for a given sensor and depends only on its material properties and geometric configuration. Therefore, the ringing frequency can be corrected by off-line filtering assuming the data has been collected at fast enough rate (~ 10 times faster than the piezo resonance is a safe rule of thumb).

The captured waveform on the FIT prototype shows a second positive phase that seems indicative of a reflection of the incoming pressure wave front. This might be due to the specific characteristics of the geometric layout used in these tests. Accurate placement of both pressure sensors in an improved test rig will help clarify the reason for this apparent reflected second peak in pressure.

The last component missing in the proposed CBI-ESP device (cumulative blast and impulse electronic sensing package) is a new data logger capable to provide sampling rate up to 1 MHz in a package no larger than 1 inch square. This is the focus of the next performance period of this subcontract.